

# **NUMERICAL INVESTIGATIONS ON RETAINING WALL SUBJECTED TO STATIC LOADS AND VIBRATIONS**

**MAJOR PROJECT – II REPORT**

**SUBMITTED IN FULFILLMENT OF THE REQUIREMENTS FOR  
THE AWARD OF THE DEGREE**

**OF**

**MASTER OF TECHNOLOGY**

**IN**

**GEOTECHNICAL ENGINEERING**

Submitted by

**NITISH KUMAR**

**2K19/GTE/10**

Under the supervision of

**PROF. ASHUTOSH TRIVEDI**



**DEPARTMENT OF CIVIL ENGINEERING**

**DELHI TECHNOLOGICAL UNIVERSITY**

(Formerly Delhi College of Engineering)

Bawana Road, Delhi – 110042

OCTOBER 2021

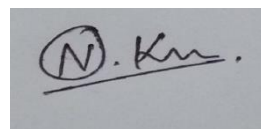
# DELHI TECHNOLOGICAL UNIVERSITY

(Formerly Delhi College of Engineering)

Bawana Road, Delhi – 110092

## **CANDIDATE'S DECLARATION**

I, **NITISH KUMAR**, roll no. **2K19/GTE/10** student of M.Tech, Geotechnical Engineering, hereby declare that the Dissertation titled “**Numerical investigations on retaining wall subjected to static loads and vibrations**” which I have submitted to the Department of Civil Engineering, Delhi Technological University, Delhi, in fulfillment of the criteria for the granting of the Master of Technology is original and has not been plagiarized without due citation. This work has never been the foundation for a degree, diploma associateship, fellowship, or other comparable title of honor.

A rectangular box containing a handwritten signature in black ink. The signature appears to be 'N. Kumar' with a stylized 'N' inside a circle and a horizontal line underneath.

**(NITISH KUMAR)**

Place: Delhi

Date: 15/10/2021

**DEPARTMENT OF CIVIL ENGINEERING**

**DELHI TECHNOLOGICAL UNIVERSITY**

(Formerly Delhi College of Engineering)

Bawana Road, Delhi – 110092

**CERTIFICATE**

I hereby certify that the Project Dissertation titled “**Numerical investigations on retaining wall subjected to static loads and vibrations**” which is submitted by NITISH KUMAR, roll no. 2K19/GTE/10 (Civil Engineering), Delhi Technological University, Delhi for achieving the criteria of awarding the Master of Technology degree, is a record of the project work carried out by the student under my supervision. This study has not been submitted partly or wholly for any diploma or degree at this University or elsewhere, to the best of my knowledge.

Place: Delhi

Date: 15/10/2021

**Prof. A. Trivedi**

**(SUPERVISOR)**

## **ABSTRACT**

In the present study, response analysis of retaining wall subjected to static and dynamic load is carried in a finite element numerical program. The well-graded, poorly graded, and clayey soil is taken in backfill to examine the backfill-retaining wall interface system. The lateral deformation at the top of the retaining wall with soil having varied densities, moduli of elasticity, and angle of internal friction are observed as 9 mm, 77 mm, and 71 mm for well-graded, poorly graded, and clayey soil respectively. For stabilization purpose, steel strips and geogrid reinforcements are introduced into the soil. In total 7 layers of steel strips and geogrids are provided separately to the system having 700 mm edge-to-edge vertical spacing. Further, frequency response is investigated on the retaining wall with a frequency sweep of 1-1000 Hz. The dynamic analysis on the retaining wall is conducted to calculate the resonant frequency by observing 6 variants of mode shapes with their respective mode frequencies. The results of the dynamic analysis show that the concrete wall retaining well-graded soil attained resonance condition at a higher frequency and thereby, stiffer than the other two considered conditions of the wall-backfill system. The results obtained in the present study are significantly improved over the results in the available literature.

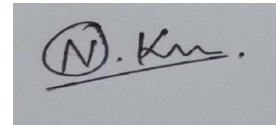
## **ACKNOWLEDGEMENT**

I express my profound gratitude to Prof. Ashutosh Trivedi, Department of Civil Engineering, Delhi Technological University, whose guidance and words of encouragement have been a great force that enabled me to prepare this project report on the topic “**Numerical investigations on retaining wall subjected to static loads and vibrations**”. He devoted considerable time to guiding me through the work and simultaneously keeping a check on the work and made valuable suggestions.

I also express my gratitude towards Ms. Nisha Soni (Ph.D. scholar, Delhi Technological University) and Mr. Yakshansh Kumar (Ph.D. scholar, Delhi Technological University) for helping me and correcting my work. They made valuable suggestions to improve my project work.

I would like to thank my parents for constantly encouraging me and being my support system throughout the work.

Date: 15/10/2021

A handwritten signature in black ink, appearing to read 'N. Kumar', is enclosed within a rectangular box.

**NITISH KUMAR**  
**(2K19/GTE/10)**

## CONTENTS

TITLE .....	i
CANDIDATE’S DECLARATION.....	ii
CERTIFICATE.....	iii
ABSTRACT.....	iv
ACKNOWLEDGEMENT.....	v
TABLE OF CONTENTS.....	vi
LIST OF TABLES.....	viii
LIST OF FIGURES.....	ix
CHAPTER 1: INTRODUCTION.....	1
1.1 GENERAL.....	1
1.2 MSE WALLS.....	3
1.2.1 Geogrid.....	4
1.2.2 Steel Strips.....	5
1.3 OBJECTIVES OF THE WORK.....	5
CHAPTER 2: LITERATURE REVIEW.....	7
2.1 GENERAL REVIEW OF THE LITERATURE.....	7
2.2 RESEARCH GAP.....	13
CHAPTER 3: METHODOLOGY AND MATERIALS.....	14
3.1 GENERAL.....	14
3.2 DYNAMIC ANALYSIS VS STATIC ANALYSIS.....	14
3.3 NUMERICAL APPROACH FOR PRESENT STUDY.....	14
3.3.1 Design Software Used.....	14
3.3.2 Parameters of the Model.....	16

3.4 TYPE OF MATERIALS USED IN THE STUDY.....	17
3.4.1 Type of Soil Used in the Study.....	17
3.4.2 Concrete Retaining Wall.....	18
3.4.3 Type of Reinforcement Used in the Study.....	18
3.4.3.1 Steel Strip Reinforcement.....	18
3.4.3.2 Geogrid Reinforcement.....	19
3.5 MODELING OF THE REINFORCEMENTS IN ANSYS.....	20
3.5.1 Modeling of Steel Strip in Ansys Workbench.....	20
3.5.2 Modeling of Geogrid in Ansys Workbench.....	21
3.6 BOUNDARY AND LOADING CONDITIONS.....	22
3.7 FREQUENCY RESPONSE OF RETAINING WALL.....	23
CHAPTER 4: RESULTS AND DISCUSSIONS.....	25
4.1 ANALYSIS AND RESULTS OF THE CURRENT STUDY.....	25
4.1.1 Analysis and Results for the Steel Strip Reinforcement.....	28
4.1.2 Analysis and Results for the Geogrid Reinforcement.....	30
4.1.3 Comparison of $G/G_{\max}$ vs Density of Various Models.....	34
4.1.4 Frequency Response Results of Retaining wall.....	36
CHAPTER 5: CONCLUSION AND RECOMMENDATIONS FOR FUTURE WORK.....	50
REFERENCES.....	52

## LIST OF TABLES

Table no	Table title	Page no
Table 1	Properties of well graded soil	17
Table 2	Properties of poorly graded soil	17
Table 3	Clay soil properties	17
Table 4	Material properties of retaining wall	18
Table 5	Chemical properties of steel strip	18
Table 6	Physical parameters of steel strip used in the study	19
Table 7	Chemical properties of the geogrid	19
Table 8	Physical properties of the geogrid	20
Table 9	Comparison of results of deformations in unreinforced and reinforced soil in different cases	31-32
Table 10	Comparison of the deformation of soil models with the steel strips and the geogrids	32
Table 11	Typical values of void ratio for different types of soil	34
Table 12	Values of P with variation of plasticity index	35
Table 13	Ratio of G and $G_{max}$ with void ratio and density for different models	35
Table 14	Different models and their mode frequencies	43
Table 15	The first fundamental frequency of the retaining wall predicted by various researchers	43
Table 16	The first fundamental frequency of the retaining wall by the current study	44
Table 17	The values of force amplitude in newtons for exciting angular frequencies in radians/second	45



## LIST OF FIGURES

<b>S. No</b>	<b>Title of figure</b>	<b>Page no.</b>
Figure 1	Classification of soil reinforcement	2
Figure 2	Representation of a mechanically stabilized earth retaining wall	4
Figure 3	Difference between uniaxial and biaxial geogrid	4
Figure 4	Representation of steel strips	5
Figure 5	Workflow chart for Ansys	15
Figure 6	Dimensions of the retaining wall and the backfill modeled in Ansys	16
Figure 7	A 3-D representation of the model showing dimensions in X, Y, and Z direction with meshing	16
Figure 8	Representation of design parameters for modeling of steel strips in design software	21
Figure 9	Representation of design parameters for modeling of geogrid in design software	22
Figure 10	Loading and boundary conditions of the model	22-23
Figure 11	Deformations results in various models	27
Figure 12	Deformations result in Model 1 with steel strip reinforcement	29
Figure 13	Deformations result in Model 2 with steel strip reinforcement	29
Figure 14	Deformations result in Model 3 with steel strip reinforcement	29
Figure 15	Deformations result in Model 1 with geogrid reinforcement	30
Figure 16	Deformations result in Model 2 with geogrid reinforcement	30
Figure 17	Deformations result in Model 3 with geogrid reinforcement	30
Figure 19	Plot of $G/G_{\max}$ vs Density of various models	36
Figure 20	Mode shape patterns with respective mode frequency for well-graded soil	37-38

Figure 21	Mode shape patterns with respective mode frequency for poorly graded soil	39-40
Figure 22	Mode shape patterns with respective mode frequency for clayey soil	42
Figure 23	Frequency response analysis of displacement for retaining wall supporting well-graded soil in semi-log scale	46
Figure 24	Frequency response analysis of displacement for retaining wall supporting poorly graded soil in semi-log scale	47
Figure 25	Frequency response analysis of displacement for retaining wall supporting clayey soil in semi-log scale	47
Figure 26	Comparison of frequency response analysis of displacement for retaining wall supporting well-graded, poorly graded, and clayey soil in log-log scale	48



# **CHAPTER 1**

## **INTRODUCTION**

### **1.1 GENERAL**

Retaining walls or structures are inherently unstable against vibrations. The vibrations can occur in a structure by the dynamic forces generated by the nature or environment by earthquake, mechanical equipment like heavy machinery work in the vicinity of the retaining structure or due to several human activities like street or highway traffic, laying of railway lines, running of trains, walls in the vicinity of the airport, etc. can cause horrendous vibrations. So, a retaining structure should be constructed or must have some arrangements, to withstand such vibrations. These vibrations can be reduced to a significant extent by reinforcing the soil with suitable reinforcements. Some widely used reinforcement materials are geosynthetics, steel, concrete, wood, thermoplastics, aluminum; strips, grids, sheets, ropes, etc.

Casagrande, presented the initial notion of reinforcing soil systems, but Henry Vidal, 1965 introduced a new way of using reinforced earth in modern soil structures as a composite material. He linked the compressive and shear strength of well-compacted granular fill with the tensile strength of reinforcing elements including steel strips, geosynthetic polymers, steel bars, and welded wire matting.

Reinforcing materials like synthetic fibers, natural fibers, thin strips of metal, micropiles, and soil nails are incorporated within the soil mass to improve its different engineering qualities. The primary idea underlying geosynthetic soil improvement is that the reinforcing materials absorb shear stresses or tensile loads within the system, avoiding shear or severe deformation failure (Patel, 2019). To enhance strength and ability to sustain higher loads, traditional soil reinforcement methods included combining straw with mud, reinforcing with woven reeds, and utilizing branches and other plant material. Modern soil reinforcement employs stronger and more lasting materials, but many of the same underlying mechanisms that produced strength in these early applications are still in use (Nicholson, 2015).

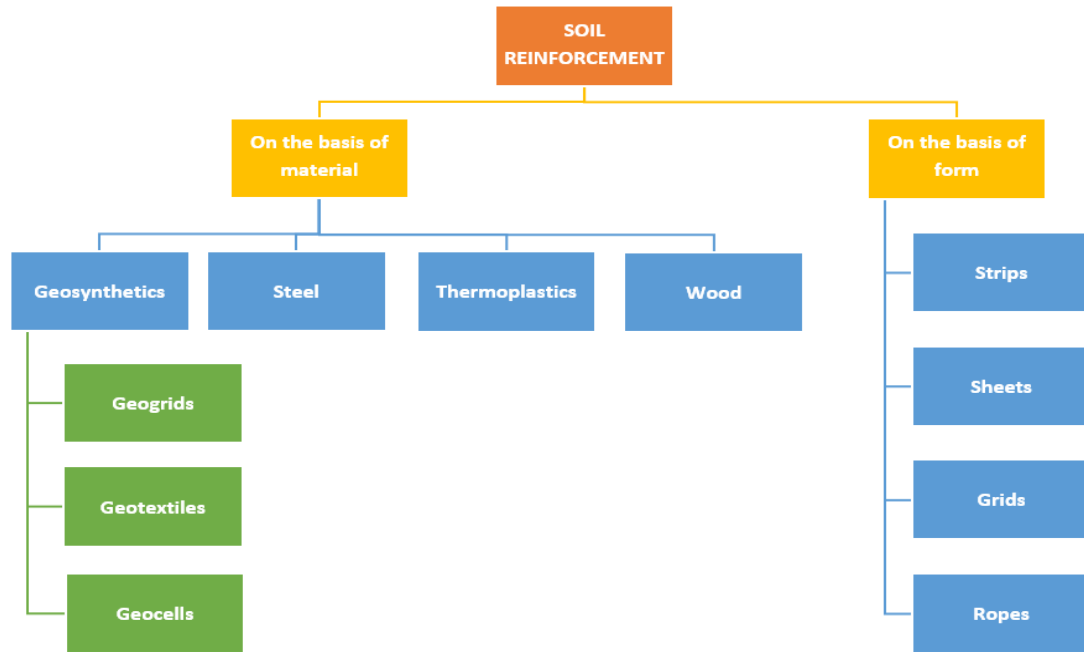


Fig. 1: Classification of soil reinforcement

The first known research of the reinforced earth walls behavior subjected to dynamic loads was reported by Richardson et al, (1975) using a shaking table. Since then various researches have been done for investigating the reinforced earth walls behavior when subjected to dynamic loads. A full-scale test on the model was conducted by Richard et al, (2015) on a 6 meters high retaining wall when the soil is reinforced with steel strips. Some recent studies are also concluded like Christopher Y. Tuan, (2014) introduced an analytical method designing of Mechanically Stabilized Embankments (MSE) walls that can withstand ground shock loading when subjected to a backfill explosion. The data from 24 m wide and 4.6 m high reinforced soil walls were reported for the analytical method, and then the accuracy had been verified by finite element method (FEM) Ansys. Christine et al, (2018) carried out four dynamic analyses to throw some light on the panel type MSE walls behavior, considering 4 m and 9 m height. The MSE walls were reinforced with steel strips and geogrid and were analyzed when subjected to surface vibration and the results were validated by Plaxis 3D software. Li et al, (2020) tried to investigate the retaining walls' dynamic responses by reinforcing it with the tires waste as well as with the geogrid simultaneously. A comparison had been done for the adopted system with that of system reinforced with tires waste, geogrid, and geocell. The magnitude of vertical earth pressures and accelerations were measured at chosen

points in the models and deformations of the various reinforced retaining walls under simulated dynamic vehicle loads were reported. Additionally, the variety of loading magnitude, speed of the vehicle, and tires spacing were also examined. Ling et al, (2004) were analyzed the dynamic behavior of geosynthetic reinforced soil retaining walls. For this they had first analyzed a full-scale wall by performing a series of 5 shaking table tests then the values were compared with Diana-Swandyne – II, a finite element method. Komakpanah et al, (2012) studied the frequency responses of soil retaining walls reinforced with polymeric strips. In the research, the authors were mainly focused on the displacement of the reinforced walls and the maximum axial force in the reinforcement, and the validation of the dynamic behavior was done by FEM FLAC 2D.

## **1.2 MSE WALLS**

The Mechanically Stabilized Earth (MSE) walls are earth retaining structures that are made up of three basic elements: backfill soil, wall facing, and reinforcement (Yang, 2008). These are used more commonly in recent decades due to their less initial cost, high ease of construction, and ability to deform without damage. These walls have been utilized for retaining walls, dams, seawalls, and bridge abutments.

These walls are widely employed in transportation systems, making them vulnerable to surface vibrations caused by driving vehicles. Because of their adaptability and flexibility to the various conditions of the site, speedy construction, great aesthetic appearance, high durability, low-cost construction, and ability to withstand deformations, and effective absorption or resistance to large vibrations, these walls are excellent solutions in urban transportation systems. As a result, MSE walls are extensively utilized as retaining walls, bridge abutments, railways in rail track beds' supporting structures, and so on, for various types of sources that cause vibrations or dynamic load (Langcuyan et al. 2018).

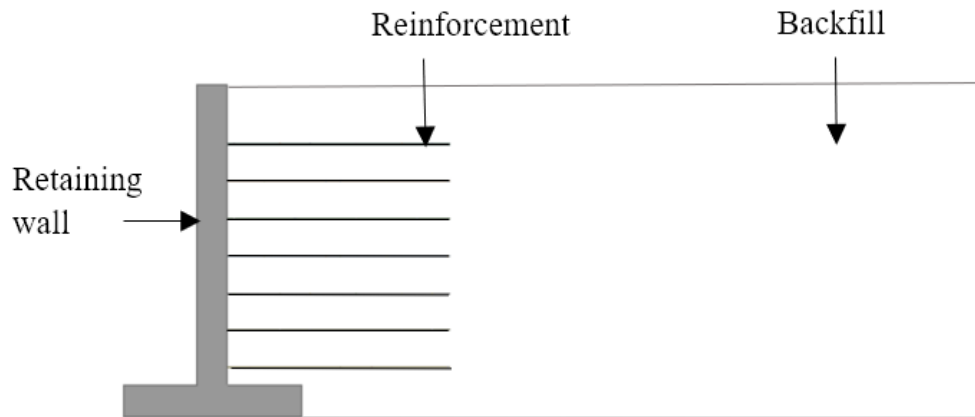


Fig. 2: Representation of a mechanically stabilized earth retaining wall

### 1.2.1 Geogrid

A geogrid is a geosynthetic (i.e., polymeric) material made up of parallelly linked sets of tensile strips with perforations large enough to enable strike-through of the surrounding earth (Das, 2016). Reinforcement and separation are their primary functions. The mechanism involved in mechanically enhancing the engineering characteristics of the composite soil/aggregate is referred to as reinforcement. The physical separation of different materials is referred to as separation.

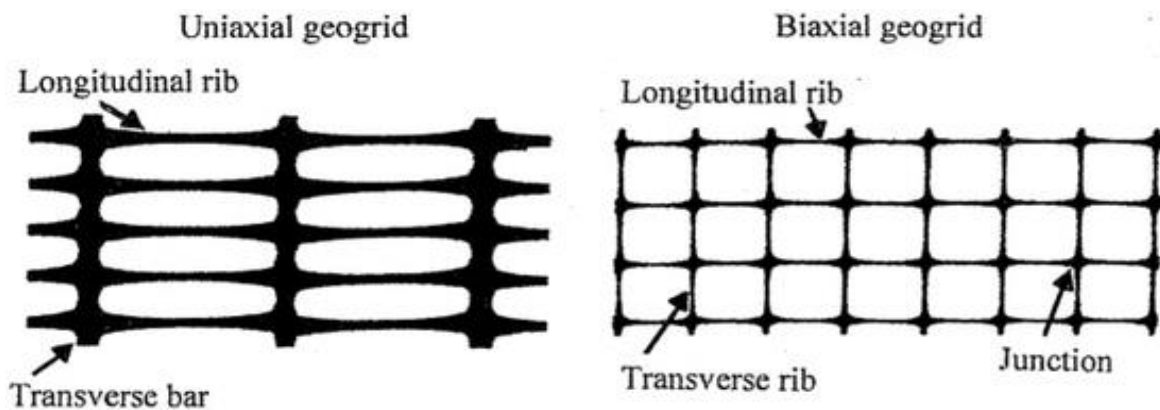


Fig. 3: Difference between uniaxial and biaxial geogrid (Das, 2016)

The two most common types of geogrids are uniaxial and biaxial geogrids. The tensile strength of the uniaxial geogrid is considered in one direction only whereas for the biaxial geogrid it is considered in two directions (i.e., machine and cross-machine

directions). These grids are composed of material ribs that are crossed or intersected in two directions during the process of manufacturing. One direction is the machine direction which as the name suggests is in the direction the same as that of manufacturing. The other direction is perpendicular to this and is known as the cross-machine direction (CMD). Amongst various geotextiles, geogrids are considered much harder and stiffer. In geogrids stresses due to loads are transferred through these junctions hence strength at a junction is essential for them to function properly. Aggregates are being held up or captured together through geogrids. Through this interlocking of aggregates, the soil becomes stabilized mechanically.

### **1.2.2 Steel Strips**

Soil reinforcement can also be done by metallic strips which include steel strips, welded wires steel bar mats, and steel anchor plates which are attached to the facing by steel rods. Strips are flexible linear elements, having a thickness less than the width. The thickness of the strips is usually in the range of 3 mm to 9 mm and the width is normally in the range of 40 mm to 120 mm. The strip may either be smooth or plain or having grooves to enhance the friction between the soil and the reinforcement.



Fig. 4: Representation of steel strips (Yazdandoust, 2017)

## **1.3 OBJECTIVES OF THE WORK**

- To study the deformation behavior of a retaining wall supporting different cases of soils under static pressure with the help of FEM software Ansys.



- To analyze the influence and effect on the deformation behavior of retaining wall by reinforcing the soil with steel strips in different types of soil with the help of FEM software Ansys.
- To study the influence and the effect of the geogrid layers on the deformation behavior of retaining wall by reinforcing the backfill with geogrids in different types of soil with the help of FEM software Ansys.
- To find out the various natural frequencies of the retaining wall supporting different types of soil with the help of FEM software Ansys.
- To study the frequency response i.e, displacement response of the retaining wall in different cases by applying the harmonic loading (frequency input) and a surcharge pressure with the help of FEM software Ansys.
- To find out the resonant frequency of the retaining wall supporting different types of soil with the help of FEM software Ansys.

## **CHAPTER 2**

### **LITERATURE REVIEW**

#### **2.1 GENERAL REVIEW OF THE LITERATURE**

Capilleri et al (2019) investigated the effect of MSE walls with polymeric strips and vertical precast concrete facing panels when subjected to harmonic loading. They conducted full-scale tests on a wall having a height of 6 m in Jundiá, Brazil for numerical modeling. The numerical and experimental findings were first compared for static loading to ensure that the numerical model was accurate, and then it was exposed to harmonic loading to examine the strains, deformations, and stresses that occurred in the geostrips under dynamic loading circumstances. They concluded that the development of reinforcing tension is unaffected by smaller acceleration situations (i.e. 0.10g).

Langcuyan et al (2018) carried out four dynamic analyses to throw some light on the behavior of panel type MSE walls, considering 4 m and 9 m height. The MSE walls were reinforced with geogrids and steel strips and were analyzed when subjected to surface vibration and the results were validated by Plaxis 3D software. They concluded that both the reinforcements produced a significantly low range of deformations and stability behavior under dynamic loads. The width of the reinforcement and pattern of arrangement play a key in the stability of MSE walls

Zhenqi et al (1995) evaluated the dynamic responses of a geosynthetic reinforced soil retaining wall by using FEM analysis. They concluded that as we increase the magnitude and duration of base excitations, the relative displacement and the shear force between modular units increase under simulated seismic events. The shear forces and relative displacements were maximum at the interface where a geosynthetic was present. They also reported that the differences in the peak acceleration distribution along the wall height were minor.

Tufan Cakir (2015) introduced a finite element approach for analyzing the dynamic behavior of cantilever walls when subjected to vibrations. He performed the dynamic

study of the cantilever wall with backfill in the time domain using the finite element method and five distinct subsoil conditions. The system's finite element model was built with the Ansys finite element software. By comparing the findings of five different soil types, it is determined that the vibration response of cantilever retaining structures is a complicated soil-structure interaction problem, and the magnitudes of wall movements and stresses generated by ground vibrations are very sensitive to the reaction of the soil underneath the wall.

Samal et al (2015) investigated the dynamic responses of pond ash when reinforced with geogrids. Block resonance tests were conducted at the ash pond area of a thermal power plant in Uttar Pradesh, India to experimentally check the efficacy of geogrid reinforcement. They concluded that with the reinforcement of geogrid layers the resonant frequency diminished by 4%, 9%, and 11% respectively when compared to unreinforced cases. The damping ratio increased by 2%, 5%, and 7% in respective cases.

Qiu et al (2019) conducted a series of simulations based on the Discrete Element Method (DEM) for showing the dynamic response of embankment reinforced with geogrid and Geogrids with Strengthened Nodes (GSN) by varying the vibration frequencies and comparing the influence of the reinforcement i.e ordinary geogrid vs Geogrids with Strengthened Nodes (GSN). The findings show that as the vibration increases, the settlement ratio tends to increase and slowly gets stable. The effect of GSN at the same frequency on restricting the settlement ratio showed better results than ordinary geogrid, but as the frequency shifted to higher levels, the reinforcing effect of ordinary geogrid and GSN both were reduced.

Safaei et al (2020) conducted the uniaxial shaking table tests to compare the behavior of ground vibrations on multi-tiered and single-tiered MSE walls by using physical modeling. For this purpose, a 10 m total height was designed in 1 m height prototype wall models. The alternating sine waves were then applied to the system with a gradual increase in their intensities in 14 typical forms. They reported that there was a decrement of about 230% in deformations in the facing of multi-tiered models as compared to single-wall models. Under different input excitations, an outward

deformation mode had introduced in the case of the single-wall model whereas multiple deformation modes occurred in the multi-tiered wall model.

Tufan Cakir (2012) investigated the dynamic behavior of a cantilever retaining wall exposed to varied ground movements. The research is divided into three sections. The finite element model with viscous boundary is suggested under a fixed-base condition in the first section. In the second section, analytical expressions are provided utilizing the modal analysis approach to offer finite element mode verification, and an acceptable agreement between numerical and analytical findings is obtained. Finally, some comparisons on lateral displacements and stress responses under varied ground movements are conducted by altering the soil characteristics. It is observed that the interaction between the soil and structure has an important influence on the behavior of the walls under vibrations.

Ling et al (2004) studied the behavior of geosynthetic reinforced soil retaining walls, dynamically. They had first analyzed a full-scale wall by performing 5 shaking table tests then the values were compared with a modified version of Diana-Swandyne – II, a finite element method. They presented lateral earth pressures values, deformations values of the wall facing, and strains values in the reinforcement layers. By comparing numerical and experimental results, they concluded that the finite element method was able to simulate the dynamic and constructional behavior as well. The results indicated that with the increase in height of the wall, for both reinforced and backfill zones, there was a slight increase in the acceleration values as well. The findings also indicated that the spacing between the reinforcements and reinforcements' length played a key role in reducing strains in the reinforcements and deformations of the wall.

Komakpanah et al (2012) analyzed the frequency responses of soil retaining walls reinforced by polymeric strips. The main focus was on the displacement of the reinforced walls and the maximum axial force in the reinforcement, and the validation of the dynamic behavior was done by FEM FLAC 2D. They reported that the natural frequency of the soil system reinforced with polymeric strips was 3 Hz. The forces in the reinforcement increase from top to bottom, so they recommended using stronger reinforcements in lower layers. On comparing, according to AASHTO standard, the displacement of the reinforced soil retaining wall with polymeric strips under different

frequencies it was analyzed that except in resonance state, all the displacements are smaller.

Wang et al (2014) studied the dynamic response of retaining wall reinforced with geogrid by conducting the shaking table tests in saturated backfill sand. They had constructed two retaining walls one with reinforcement and the other without reinforcement to study the usefulness of geogrids in the saturated sand under vibrations. They investigated lateral displacements of walls, wall accelerations, and settlements of the saturated backfill sand. They concluded that the geogrid layers were still successful in reducing wall deformations in saturated soils since the reinforced wall model's lateral displacements were smaller than the unreinforced wall model's. The acceleration responses, backfill surface settlements, and other characteristics of the reinforced wall model were smaller or weaker than those of the unreinforced wall model for all excitations.

Yazdandoust (2017) performed experimental studies to investigate the effect of steel-strip reinforced soil retaining walls under ground vibrations. Five wall models were constructed and examined for a series of uniaxial shaking table tests by varying the strip lengths on a reduced scale under different input motion parameters. It was observed that by reducing the length of the strips from 0.7 times the height of the wall to 0.5 times the height of the wall, the bulging deformation mode overpowered the prominent character of rotation mode. So the mode of deformation depends greatly on the length of the strips. It was also found that acceleration amplification factors directly depended on peak accelerations as they increased with increasing the peak acceleration magnitude.

Tuan (2014) introduced a simple analytical method that explained the designing of MSE walls to resist ground shock loading when subjected to the vibrations due to explosion in the backfill. In this, data for reinforced soil walls having 4.6 m height and 24 m width were reported for the analytical method, and then the accuracy had been verified by FEM (Ansys). For a set of tests, they concluded that the average of loading wave velocity was 306 m/s and the average of acceleration was reported as 19g.

Li et al (2020) investigated the retaining wall's dynamic response by reinforcing it with the tires waste and geogrid simultaneously. A comparison had been done for the adopted system with that of the system reinforced with geocell, tires waste, and geogrid.

The magnitude of vertical earth pressures and accelerations were measured within the model and deformations of the various reinforced retaining walls under dynamic vehicle loads were reported. They concluded that the tires and geogrids reinforcement gave better results than commonly used reinforcement materials like geogrids & geocells. On comparing tire geogrid reinforcement with biaxial geogrids, the deformation of the retaining wall panel ceased by 30%, peak acceleration reduced by 27%, and peak earth pressures reduced by 30%. On comparing tire geogrid reinforcement with geocells the deformation of the retaining wall panel ceased by 20%, peak acceleration reduced by 16%, and peak earth pressures reduced by 13%.

Hussaini et al (2020) conducted a series of experiments to investigate the influence of loading frequency on the deterioration and deformation behavior of ballast with and without geogrids. Five geogrids were utilised, each with a distinct aperture size and shape. Fresh granite ballast with a  $D_{50}$  (mean particle diameter) of 42 mm was used, as well as sub-ballast with a  $D_{50}$  of 3.5 mm. The tests were conducted on a frequency sweep of 10 to 40 Hz. This study concluded that the lateral settlement, as well as vertical settlement in ballast and sub-ballast, decreases linearly with an increase in frequency. It also showed that the degree of deformations in both sub-ballast and ballast reduced considerably upon the inclusion of geogrids.

Khati et al (2012) experimentally studied the dynamic behavior of foundation on reinforced and unreinforced sand beds. They carried out experimental investigation on model concrete blocks. A total 36 number of vibration tests were conducted on reinforced and unreinforced sand beds with the evaluation of embedment effect. From the study, it can be concluded that for a constant embedment ratio, the maximum amplitude increases significantly with an increase in the level of the exciting force whereas the magnitude of resonant frequency decreases for both reinforced and unreinforced sand.

Chowdhury et al (2015) tried to forecast the behavior of a gravity wall with a generalized backfill. They considered five cases to study the behavior of retaining wall. For the first case, they took wall retaining cohesionless soil only. For the second case, they took an inclined wall retaining cohesionless soil. They considered the third case as wall retaining soil possessing  $c$  and  $\Phi$  parameters. Likewise 2 more cases. Finally, the

results of time-periods and the first three mode shapes are compared to a 2-D finite element analysis Ansys and validation was also done by Ansys. From the findings, it can be concluded that the suggested methods' time-periods are in excellent agreement with those derived using Ansys. It has been observed that when the stiffness of the foundation is less than the stiffness of the structure, there is an amplification of the response.

Darvishpour et al (2016) presented analytical formulas for determining the natural frequencies of the retaining wall. A stiffness ratio parameter was defined in this work, and it was demonstrated that raising this ratio leads the soil-wall system to stiffen and raises the frequency. A good agreement was found in vibration modes of the retaining wall when the suggested technique's findings were compared to the results from the finite element method. Meanwhile, a discrepancy was discovered when the suggested method's results were compared to the results of prior studies. As the results demonstrate, raising the height of the wall has a greater influence on the fundamental frequency of the wall.

A reinforced concrete retaining wall and its supporting backfill soil were subjected to a dynamic full-scale test by Elgamal et al (1996). A frequency sweep test was performed to evaluate the response of the soil-wall system over a wide range of resonances. Measurements of acceleration were taken throughout the length of the wall and on the backfill surface. They chose a wall backfill system in the campus of a New York institute. They concluded that the retaining walls exhibit resonant configurations with motion variation over the length and height of the wall. For typical seismic excitation circumstances with height less than or equal to 10 m, modal damping of 5% may be regarded as a cautious estimate.

Dongare et al (2019) aim to create a structurally efficient retaining wall profile by comparing it to a cantilever retaining wall having the same height and characteristics, which is then evaluated using the finite element technique and Ansys software under static loading conditions. This gravity retaining wall may be seen in Karjat, Maharashtra, India. Then, using finite element software (Ansys), a model is created and the behavior of the retaining wall for deformation and displacement is calculated for the static load. They did the calculations for both types of retaining walls manually with all

necessary checks. In the case of gravity retaining wall, the factor of safety for overturning was found to be 3.45 ( $> 1.5$ , therefore, safe), the factor of safety (FOS) for sliding was found out to be 1.47 ( $< 1.5$ , therefore, fails, the shear key provided). In the case of the cantilever retaining wall FOS for overturning was 3.48 (safe) and for sliding, FOS comes out to be 1.53 (safe). Finally, it was determined that a cantilever retaining wall is the best solution available.

## **2.2 RESEARCH GAP**

In previous studies, researchers have analytically investigated the dynamic behavior of the retaining walls. The papers are also available when the retaining walls with reinforced soil backfill are subjected to ground and surface vibrations, experimentally. However, the numerical investigations on the retaining walls under vibrations have not been studied to a great extent. Also, the numerical investigations on the retaining walls, retaining different cases of soil as a backfill material are below par. The numerical investigations on the retaining walls supporting different cases of the soil when reinforced with 2 different kinds of reinforcement materials are even less. Moreover, the frequency response analysis of the retaining walls with different cases of the soil under harmonic loading is exiguous.



## **CHAPTER 3**

### **METHODOLOGY AND MATERIALS**

#### **3.1 GENERAL**

This chapter accounts for the numerical approach that is used for the present study, different kinds of materials along with their properties, and the boundary as well as loading conditions involved. For the numerical approach, simulation software Ansys is used. The three main types of materials considered in the study are soil (well-graded, poorly graded, clayey), concrete retaining wall, and reinforcement (steel strips and geogrids). The modeling of the steel strips and geogrids is also discussed in this section.

#### **3.2 DYNAMIC ANALYSIS VS STATIC ANALYSIS**

A dynamic analysis is different from a static analysis by the fact that the dynamic analysis takes into consideration the forces, basically, inertial forces, induced by the rigid body motions and the three trio namely deformation, velocity, and acceleration instead of considering only the elastic forces caused due to deformations. The illustration of this difference can be given by the following equation of the Finite Element Model :

$$[K] \times [x] = [F] \quad (3.1)$$

$$[M]\{\ddot{x}\} + [C]\{\dot{x}\} + [K]\{x\} = [F] \quad (3.2)$$

The term  $[K] \times [x]$  in eq 3.1 and 3.2, refers to the stiffness matrix multiplied by the displacement vector associated with the stiffness matrix.  $[F]$  is the externally applied force vector. The extra terms in the eq 3.2 are inertial force,  $[M]\{\ddot{x}\}$  and  $[C]\{\dot{x}\}$  which is the damper force. These two are dynamic forces terms that distinguish dynamic simulations from static simulations. Since this study involves loads that are changing rapidly (vibration motion caused by harmonic loading), a considerable amount of accelerating or deaccelerating motions will be developed, hence inertial forces will be there and dynamic analysis is required to capture their effects.

#### **3.3 NUMERICAL APPROACH FOR PRESENT STUDY**

##### **3.3.1 Design Software Used**

For the analysis of the present study, Ansys Workbench 2021 version is used. The Ansys is a multi-functional analysis programming tool that can be used for a wide range of engineering fields for analysis of deformations, strain, stresses, etc. The basic workflow of the Ansys which is used for designing and simulation of the models is given below in Fig. 5 in the form of a flowchart.

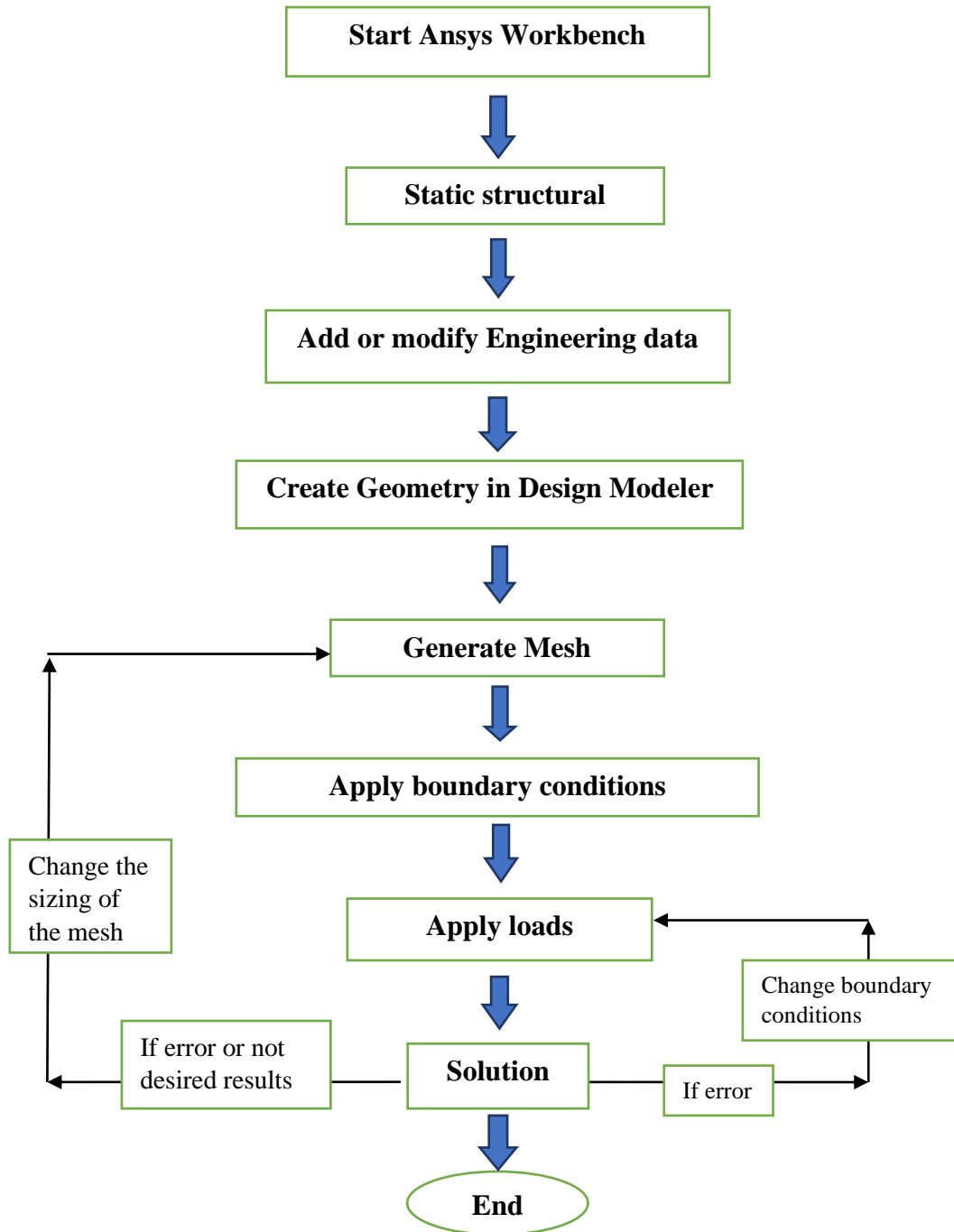


Fig 5: Workflow chart for Ansys

### 3.3.2 Parameters of the Model

The basic dimensions of the model used in this study are the same which were taken by Sridevi et al (2021). A retaining wall having a height of 6.25 m (Y-Axis) is modeled in Ansys. The length of the retaining wall is taken as 15 m (Z-axis). The base width of the retaining wall is taken as 3.5 m and the slab thickness is considered as 0.6 m. The length of the backfill is considered as 18 m (X-axis). A pictorial Parameters of the model along with dimensions is presented in Fig. 6.

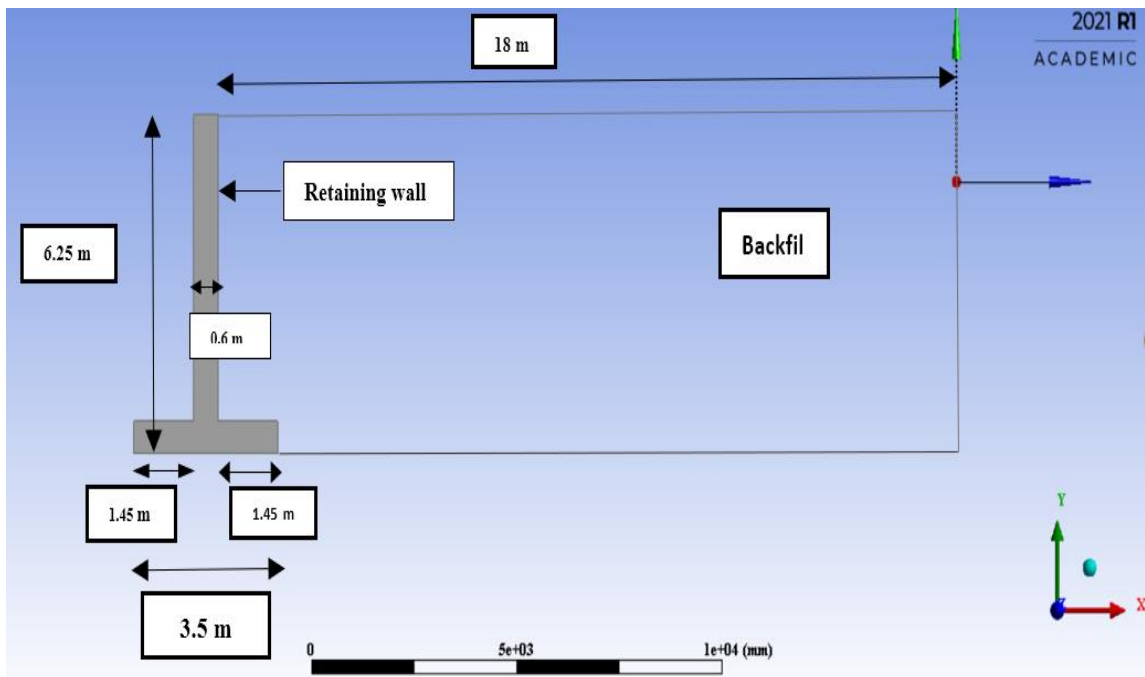


Fig. 6: Dimensions of the retaining wall and the backfill modeled in Ansys

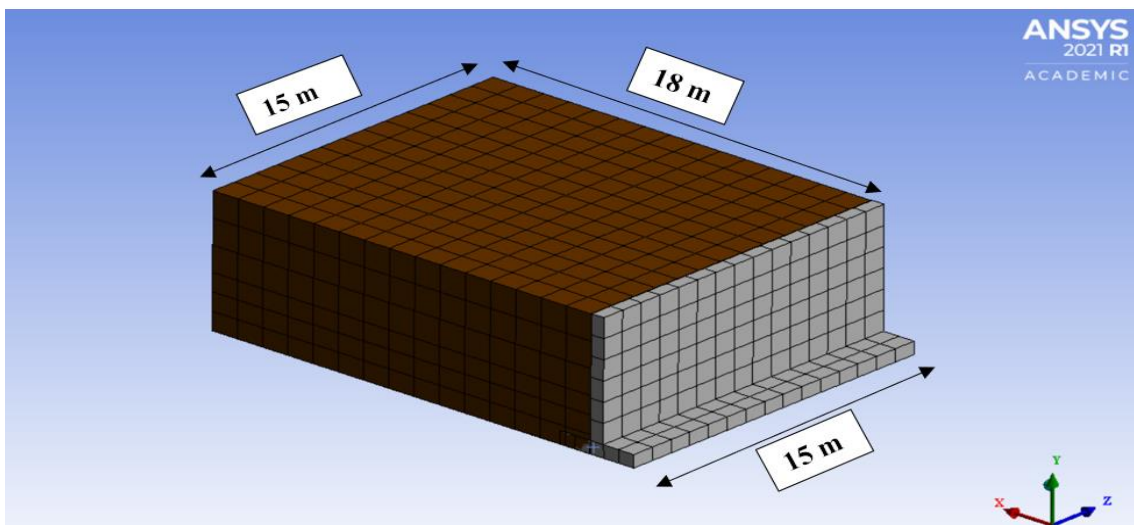


Fig. 7: A 3-D representation of the model showing dimensions in X, Y, and Z direction with meshing

### 3.4 TYPE OF MATERIALS USED IN THE STUDY

For this study, three main types of materials are considered viz., soil (as a backfill), concrete (retaining wall), and reinforcements.

#### 3.4.1 Type of Soil Used in the Study

The soil is considered homogeneous and isotropic. The backfill is considered in a dry state i.e, no effect of the water table is taken into account. For this study 3 types of soil are considered namely, well-graded soil, poorly graded soil, and clayey soil. The properties of all three types of soil are taken from Sridevi et al (2021) and are summarized below.

Table 1: Properties of well-graded soil (Sridevi et al 2021)

S. No.	Property	Magnitude
1.	Density (kN/m <sup>3</sup> )	20.4
2.	Modulus of elasticity (kN/m <sup>2</sup> )	8 x 10 <sup>4</sup>
3.	Poisson's ratio	0.3
4.	Angle of internal friction (degree)	35

Table 2: Properties of poorly graded soil (Sridevi et al 2021)

S. No.	Property	Magnitude
1.	Density (kN/m <sup>3</sup> )	19.4
2.	Modulus of elasticity (kN/m <sup>2</sup> )	8 x 10 <sup>3</sup>
3.	Poisson's ratio	0.3
4.	Angle of internal friction (degree)	23

Table 3: Clay soil properties (Sridevi et al 2021)

S. No.	Property	Magnitude
1.	Density (kN/m <sup>3</sup> )	18.4
2.	Modulus of elasticity (kN/m <sup>2</sup> )	7 x 10 <sup>3</sup>
3.	Poisson's ratio	0.3
4.	Angle of internal friction (degree)	18

### 3.4.2 Concrete Retaining Wall

The retaining wall used for this analysis is modeled as a concrete retaining wall with a uniform cross-section throughout. The properties of the concrete retaining wall are summarized below.

Table 4: Material properties of retaining wall (Sridevi et al 2021)

S. No.	Property	Magnitude
1.	Density (kN/m <sup>3</sup> )	24
2.	Modulus of elasticity (kN/m <sup>2</sup> )	27386 x 10 <sup>3</sup>
3.	Poisson's ratio	0.2

### 3.4.3 Type of Reinforcement Used in the Study

The two types of reinforcements used in the study are steel strips and geogrids. The properties of both the reinforcements and the design parameters considered are described below one by one in detail.

#### 3.4.3.1 Steel Strip Reinforcement

The data for the chemical properties of the steel strip that were used by Yazdandoust (2017), is taken for the present study analysis.

Table 5: Chemical properties of steel strip (Yazdandoust, 2017)

S. No.	Properties	Value
1.	Density (kN/m <sup>3</sup> )	78.5
2.	Modulus of elasticity (kN/m <sup>2</sup> )	2 x 10 <sup>8</sup>
3.	Poisson's ratio	0.3
4.	Normal stiffness (kN/m)	100 x 10 <sup>3</sup>

The physical parameters for the steel strip for the present study are different from Yazdandoust's study. A brief difference between the physical properties of the two studies is summarized here. In Yazdandoust's study, the width of the strip was 0.675 m, with thickness considered as 2.3 mm. For the present study 50 mm width, 6 mm

thickness is considered. “The standards and specifications for reinforced soil retaining walls almost always recommend a minimum reinforcing length. For example, the American Association of State Highway and Transportation Officials (AASHTO) and the Federal Highway Administration (FHWA) recommended the minimum length of the reinforcement as  $0.7 H$ ” (Komakpanah, 2012, Xu, 2019). The maximum vertical spacing should be limited to 80 cm or  $2B$ , where,  $B$  is concrete slab thickness, whichever is less (Tuan, 2014). Since the slab thickness that is considered here is 60 cm, so  $2B = 120$  cm. So maximum vertical spacing is limited to 80 cm. Therefore 70 cm vertical spacing is taken for the analysis.

Table 6: Physical parameters of steel strip used in the study

S. No.	Parameters	Value
1.	Width (mm)	50
2.	Thickness (mm)	6
3.	Length (mm)	$0.7 \times H = 0.7 \times 6250 = 4375$
4.	Horizontal spacing (mm)	300
5.	Vertical spacing (mm)	700

#### 3.4.3.2 Geogrid Reinforcement

The geogrid data for the chemical properties that were used in the analysis by Ling et al (2004), is taken for the current study purpose.

Table 7: Chemical properties of the geogrid (Ling et al, 2004)

S. No.	Properties	Value
1.	Density ( $\text{kN/m}^3$ )	11
2.	Modulus of elasticity ( $\text{kN/m}^2$ )	$30 \times 10^3$
3.	Poisson's ratio	0.316
4.	Normal stiffness ( $\text{kN/m}$ )	2500

The differences are there between the physical properties of the geogrids. They considered the thickness of the geogrid as 0.2 mm but this study used 2 mm thickness

geogrid which defines the field condition more accurately. The length and vertical spacing are also different and are considered the same as that of steel strips.

Table 8: Physical properties of the geogrid

S. No.	Parameters	Value
1.	Length of the geogrid (mm)	$0.7 \times H = 0.7 \times 6250 = 4375$
2.	Thickness of the geogrid (mm)	2
3.	Vertical spacing between two layers of geogrid (mm)	700

### 3.5 MODELING OF THE REINFORCEMENTS IN ANSYS

#### 3.5.1 Modeling of Steel Strip in Ansys Workbench

For modeling of steel strips, a strip of length 4375 mm, width 50 mm, and thickness 6 mm is sketched in ‘geometry’ of Ansys keeping 1000 mm (1 m) distance from the bottommost surface of the soil. After sketching a strip, then by using the ‘translate’ command, move the strip by 13625 mm (18000 mm – 4375 mm = 13625 mm) and used the ‘slice material’ command to build connections of the reinforcement to the concrete wall. After moving the steel strip and building connections to the wall, we create a ‘pattern’ from the ‘create’ command for horizontal spacing of reinforcement of 300 mm end to end. We enter 300 mm in the ‘offset’ row and 48 copies in the ‘copies’ row.

The total length for which reinforcement is to be provided = 15000 mm

Nominal cover from both sides = 300 mm

Therefore, total available length for reinforcement = 15000 – 300 – 300 = 14400 mm

So the number of strips required in one layer =  $\frac{\text{Available length}}{\text{Spacing}} = \frac{14400}{300} = 48$  strips

Now our bottommost reinforcement layer keeping 1000 mm distance from the bottommost soil surface and having 300 mm end-to-end horizontal spacing is modeled in Ansys. Now, for vertical spacing of 700 mm, subtracting 1000 mm from the top, we left with only 4250 mm height of the wall.

Therefore, number of reinforcement layers =  $\frac{\text{Available length}}{\text{Spacing}} = \frac{4250}{700} = 6.07$  i.e, 6 layers

Therefore total reinforcement layers = 1(already prepared) + 6 (additional layers) = 7 layers i.e, total 7 layers of reinforcement should be provided.

So to provide additional 6 layers, we again use the ‘pattern’ command. This time we enter 700 mm in the ‘offset’ row and 6 copies in the ‘copies’ row. This is how modeling of steel strip reinforcement is done in Ansys.

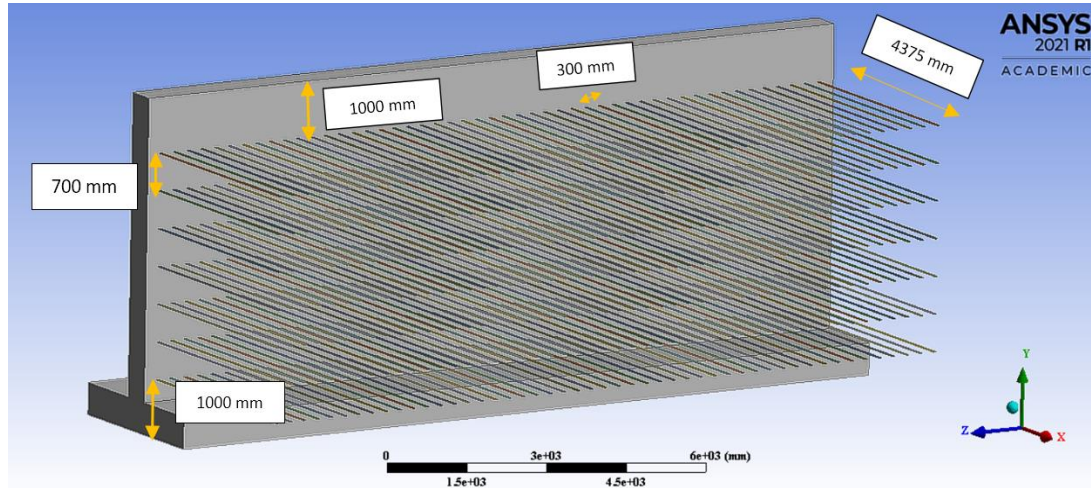


Fig. 8: Representation of design parameters for modeling of steel strips in design software

### 3.5.2 Modeling of Geogrid in Ansys Workbench

The modeling of geogrid is half the same as of steel strips. In geogrid, we have to show a net or mesh-like material. So after entering the chemical properties of geogrid in ‘engineering data’ from Table 7, we first sketch 2 mm in the Z-direction and 2 mm in the Y-direction and extrude for 4375 mm in the X-direction. Then use the ‘translate’ command followed by creating ‘pattern’ in the Z-direction for horizontal spacing followed by creating ‘pattern’ in the Y-direction for vertical spacing. To show a mesh-like object, a sketch of 2 mm in the X-direction and 2 mm in the Y-direction is drawn and extrude for 14400 mm in the Z-direction. Enter 30 mm in the ‘offset’ row and 480 copies in the ‘copies’ row for horizontal layers. Enter 700 mm in the ‘offset’ row and 6 copies in the ‘copies’ row for vertical layers.



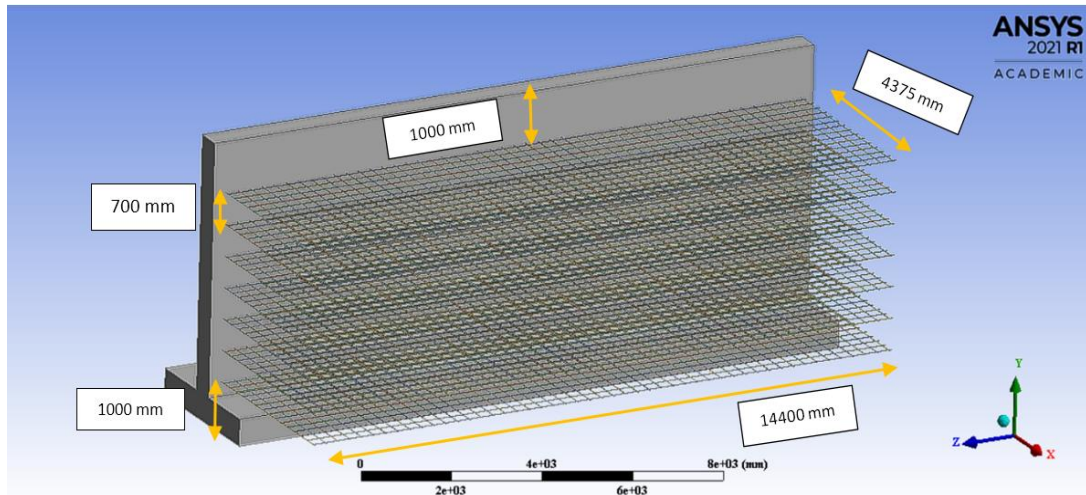
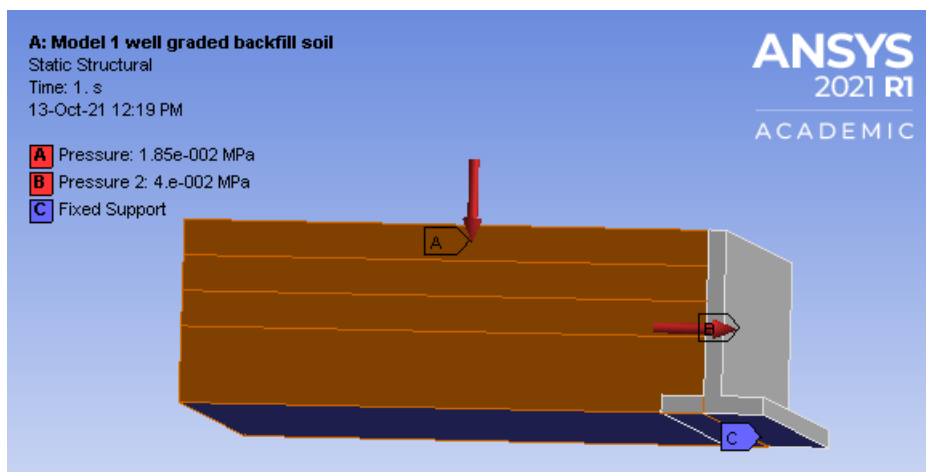


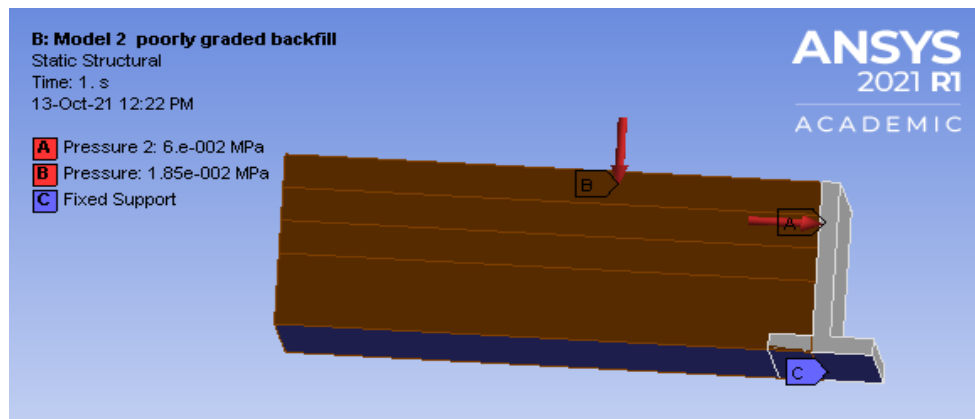
Fig. 9: Representation of design parameters for modeling of geogrid in design software

### 3.6 BOUNDARY AND LOADING CONDITIONS

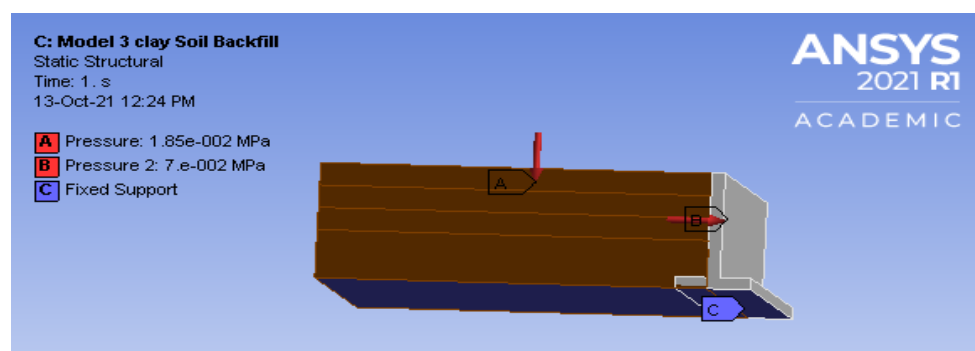
For the present study, a  $18.5 \text{ kN/m}^2$  pressure is applied on the top surface of the model which is uniformly distributed on the surface and acts as a surcharge. To add the gravitational effect and the effect of the pressure exerted by the soil mass on the retaining wall, pressure having a magnitude of  $40 \text{ kN/m}^2$ ,  $60 \text{ kN/m}^2$ , and  $70 \text{ kN/m}^2$  is also applied in the respective models, shown in Fig. 10 (a, b, c). The load and pressure analysis and calculations are shown in Ch- 4. The retaining wall and the backfill are fixed from the base and deformations are allowed in the X-direction.



(a) Loading and boundary conditions in well-graded soil (model 1)



(b) Loading and boundary conditions in poorly graded soil (model 2)



(c) Loading and boundary conditions in clayey soil (model 3)

Fig. 10: Loading and boundary conditions considered in different models

### 3.7 FREQUENCY RESPONSE OF RETAINING WALL

When no damping or driving force is applied to the system, the system tends to vibrate or oscillate at its inherent frequency, known as natural frequency. The natural frequency is also known as eigenfrequency or mode frequency. When an object or a system vibrates at a frequency that is equal to its mode frequency, the amplitude of the vibration increases considerably, perhaps causing irreversible damage.

Modal analysis is a basic method for calculating the system's inherent frequencies so that we may determine which frequencies are damaging and dangerous to it. It is the simplest analysis and it tells us that what our geometry's "resonance frequencies" are. This analysis is not tied to a loading, i.e., in modal analysis, no load is necessary, all that is required is the geometry. The geometry of the model and its constrained parameters influence the resonance frequencies. It also aids in the identification of vibration modes

and the frequencies at which they are triggered. Theoretically, the number of vibration modes is limitless, but in practice, we only want to get the ones that cause the most deformation. The modal analysis provides no information regarding the actual deformation caused by stimulation of one of those modes. The data from the modal analysis will help in performing forced vibration. When it comes to dynamic analysis, modal analysis is just the start.

When we perform modal analysis on a system we try to find out what are the natural frequencies of the system that makes it resonate. After getting the natural frequencies if we excite our model or particular object at these dangerous frequencies, how much deformation will we obtain, can be accomplished by time response dynamic analysis or frequency response dynamic analysis. When we do frequency response, we want how the system will behave in a certain defined range of frequencies and load.

## CHAPTER 4

### RESULTS AND DISCUSSIONS

#### 4.1 ANALYSIS AND RESULTS OF THE CURRENT STUDY

For the current study analysis, the dimensions and properties of the retaining wall and the backfill data are taken from Sridevi et al (2021). A total three models are prepared for this study. Model 1 is the retaining wall supporting well-graded soil as a backfill material. Model 2 is the retaining wall with poorly graded soil as a backfill material. Model 3 is the retaining wall with clayey soil backfill. After preparing all the models in the Ansys, a pressure of magnitude  $18.5 \text{ kN/m}^2$  is applied in it as a surcharge pressure. Considering a practical example of a vehicle, let's say a passenger car, having dimensions  $3 \text{ m} \times 1.5 \text{ m}$  (L x B) is parked in an area which is in the vicinity of a concrete retaining wall. The parking area is  $15 \text{ m} \times 18 \text{ m}$  that is  $270 \text{ m}^2$ . Now, area of 1 car =  $3 \text{ m} \times 1.5 \text{ m} = 4.5 \text{ m}^2$ . Let 50 cars are parked in the given area. Therefore,  $4.5 \text{ m}^2 \times 50 = 225 \text{ m}^2$ , which is the area covered by 50 cars on the given  $270 \text{ m}^2$  parking area.

As per IRC: 3-1983, the axle weight for single wheels shall not exceed 6 tonnes. Therefore for the current study, it is taken as 5 tonnes. The passenger car has 2 axles. So for 2 axles, the total weight is 10 tonnes.

Weight of 1 passenger car,  $W = 10 \text{ tonnes} = 10,000 \text{ kg}$

Load exerted by one car on the ground,  $F$

$$\begin{aligned} F &= \text{Weight (W)} \times \text{Acceleration due to gravity (g)} \\ &= 10,000 \times 9.8 \end{aligned} \tag{4.1}$$

$$F = 98,000 \text{ N} = 98 \text{ kN}$$

Therefore load exerted by 50 cars on the ground,  $F_t = 50 \times 98 \text{ kN} = 4900 \text{ kN}$

Assuming this load acts on the entire area of the backfill.

Therefore, pressure exerted by 50 cars on the given area,  $P = 4900 \text{ kN} / 270 \text{ m}^2$

$$P = 18.5 \text{ kN/m}^2$$

This pressure will act as a surcharge.

Now pressure exerted by soil due to self-weight is given by the equation,

$$P_a = K_a * \gamma * Z \quad (4.2)$$

where,

$P_a$  = Active earth pressure (kN/m<sup>2</sup>)

$K_a$  = Active earth pressure coefficient =  $\frac{1 - \sin \phi}{1 + \sin \phi}$ , where  $\phi$  = angle of internal friction

$\gamma$  = Unit weight of the soil (backfill) (kN/m<sup>3</sup>)

$Z$  = Height of the retaining wall (m)

The soil parameters that are considered in the model, are taken here also for the analysis.

For well-graded soil,  $\gamma = 20.4$  kN/m<sup>3</sup> and  $\phi = 35^\circ$ . By putting these values in eq 4.2, we get,

$$P_a = \left( \frac{1 - \sin 35}{1 + \sin 35} \right) * 20.4 * 6.25 = 40 \text{ kN/m}^2$$

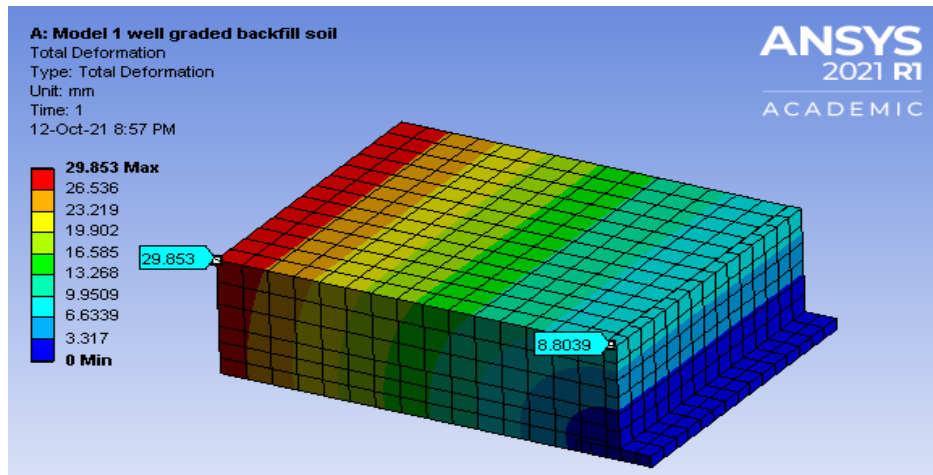
For poorly graded soil,  $\gamma = 19.4$  kN/m<sup>3</sup> and  $\phi = 23^\circ$ . By putting these values in eq 4.2, we get,

$$P_a = \left( \frac{1 - \sin 23}{1 + \sin 23} \right) * 19.4 * 6.25 = 60 \text{ kN/m}^2$$

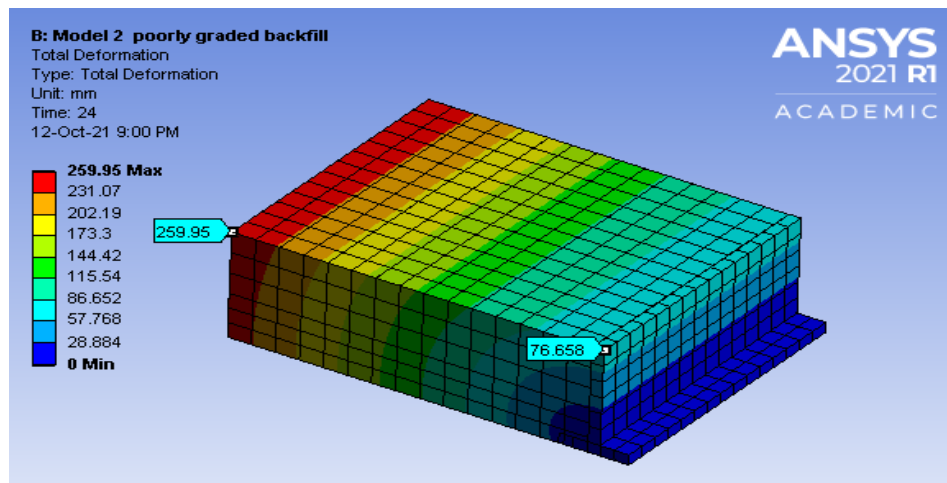
For clayey soil,  $\gamma = 18.4$  kN/m<sup>3</sup> and  $\phi = 18^\circ$ . By putting these values in eq 4.2, we get,

$$P_a = \left( \frac{1 - \sin 18}{1 + \sin 18} \right) * 18.4 * 6.25 = 70 \text{ kN/m}^2$$

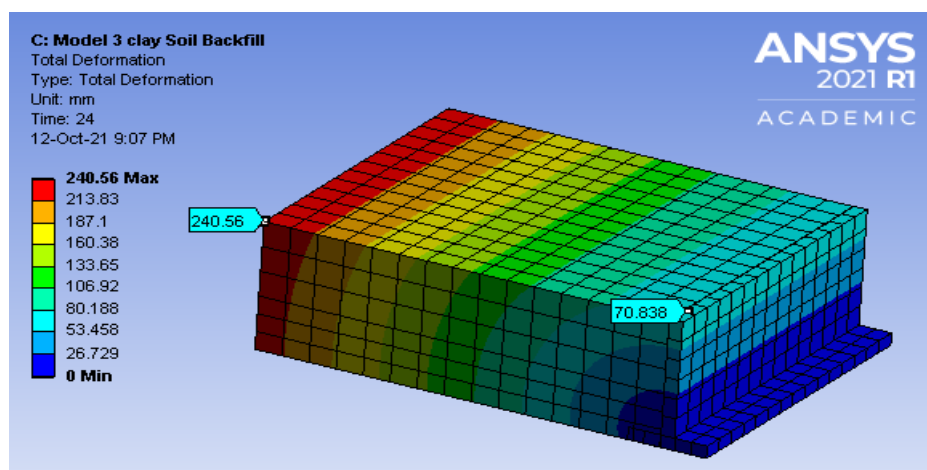
So 18.5 kN/m<sup>2</sup> pressure which will act due to 50 passenger cars parked on the given area and 40 kN/m<sup>2</sup>, 60 kN/m<sup>2</sup>, and 70 kN/m<sup>2</sup> pressure that the soil will exert due to its self-weight on the retaining wall are applied in respective soil conditions or models and then the results of deformations are calculated in the Ansys.



(a) Result for deformations in model 1



(b) Result for deformations in model 2



(c) Result for deformations in model 3

Fig. 11: Deformations results in various models

From Fig. 11, it can be stated that in model 1 which is of concrete retaining wall with well-graded soil, the maximum deformation of 29.85 mm occurred at the farthest point from the retaining wall and 8.80 mm deformation occurred at the face of the wall. In the case of model 2 i.e, poorly graded soil case, the maximum deformation of 259.95 mm occurred at the farthest point from the retaining wall which is 770% more than the well-graded soil case, and 76.65 mm deformation occurred at the wall face, which is again 770% more than the case of well-graded soil. For model 3 which is the clayey soil case, the maximum deformation of 240.56 mm occurred at the farthest point from the retaining wall and 70.83 mm deformation occurred at the wall face, which is 705% more for both the positions than well-graded soil case. To lower these deformations, soil reinforcement plays a key role. The combination of a system containing a retaining wall, backfill, and reinforcement material is commonly known as Mechanically Stabilized Earth walls or simply MSE walls. There are many reinforcement materials like geocells, wood, steel strips, geogrids, etc., out of these, steel strips and geogrids are used as reinforcement material for this study since in the real world they are most widely used as reinforcement material and their modeling is more convenient than other reinforcement materials.

#### **4.1.1 Analysis and Results for the Steel Strip Reinforcement**

After the modeling of the steel strip as discussed in section 3.5.1, we move to ‘model’ in the main window of the Ansys workbench for the analysis part. In ‘model’, the first step is to mesh the model. After meshing, apply for fixed support, and pressure to the system, from ‘static structural’. The wall is fixed at the base. Then 18.5 kN/m<sup>2</sup> pressure is applied on the top of the backfill. There will also be an effect of the dead load of the soil into the system, so again pressure is adopted from ‘static structural’ having a magnitude of 40 kN/m<sup>2</sup>, 60 kN/m<sup>2</sup>, and 70 kN/m<sup>2</sup> in respective models to incur the effect of dead load of the soil on the retaining wall. Then solutions for deformations due to applied loads are carried out in all three cases of the backfill soil and the results are shown below.

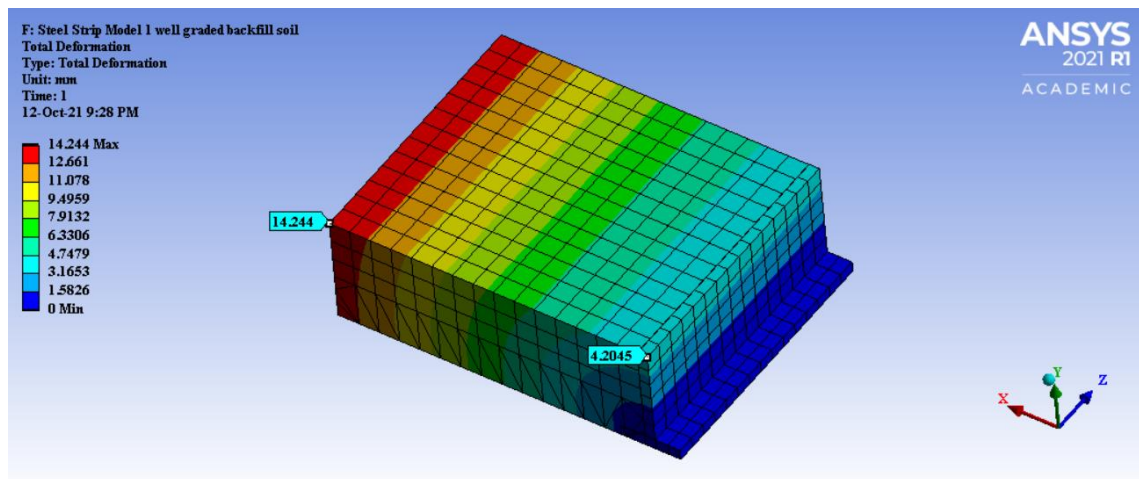


Fig. 12: Deformations result in model 1 with steel strip reinforcement

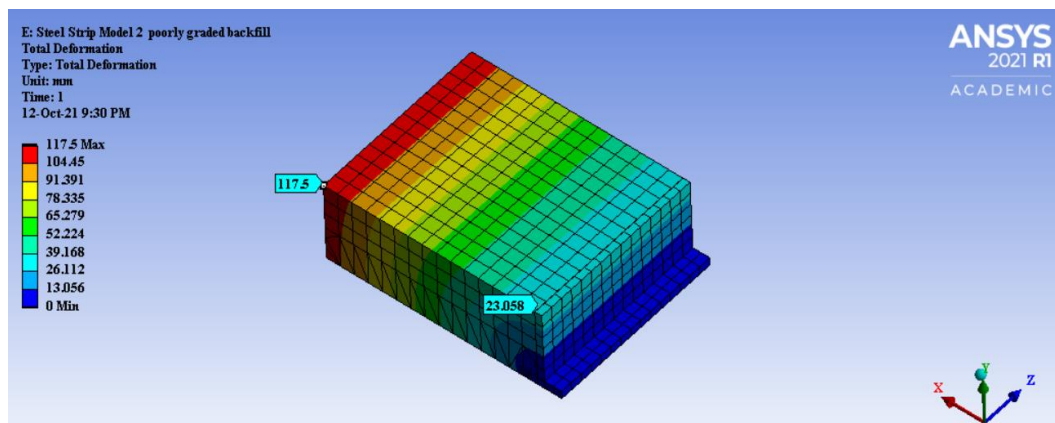


Fig. 13: Deformations result in model 2 with steel strip reinforcement

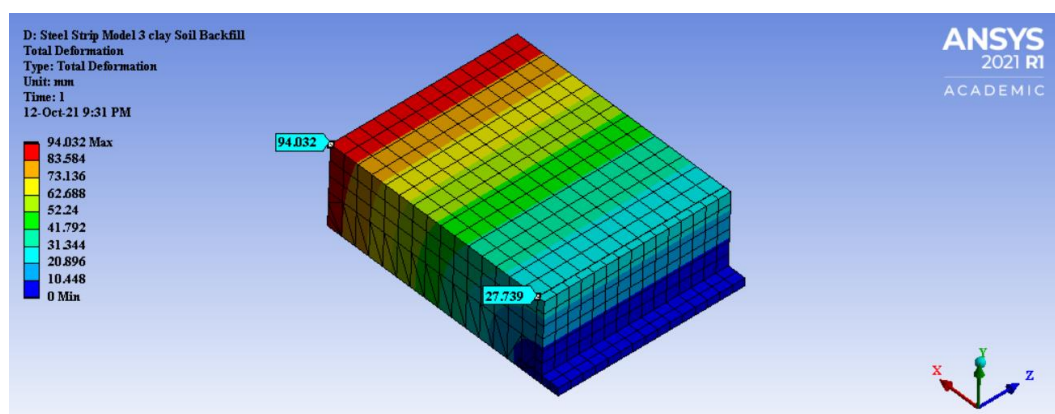


Fig. 14: Deformations result in model 3 with steel strip reinforcement



#### 4.1.2 Analysis and Results for the Geogrid Reinforcement

After the modeling of geogrid as discussed in section 3.5.2, we go for the analysis of the geogrid reinforcement. The procedure for the analysis of the geogrid reinforcement is the same as that for steel reinforcement that is discussed already. The results obtained after the analysis are shown below for all the 3 models.

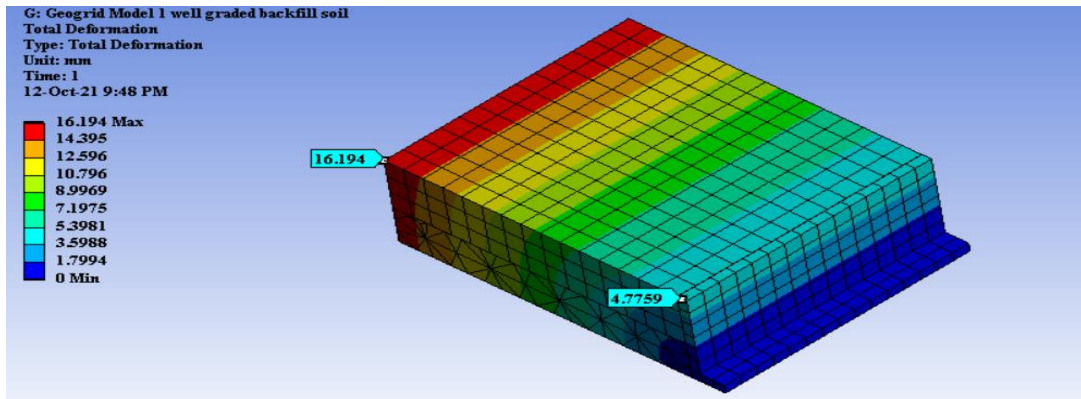


Fig. 15: Deformations result in model 1 with geogrid reinforcement

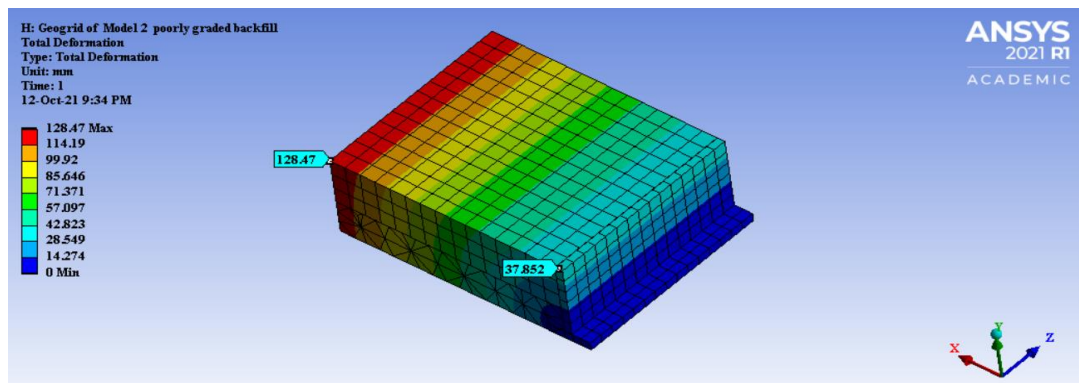


Fig. 16: Deformations result in model 2 with geogrid reinforcement

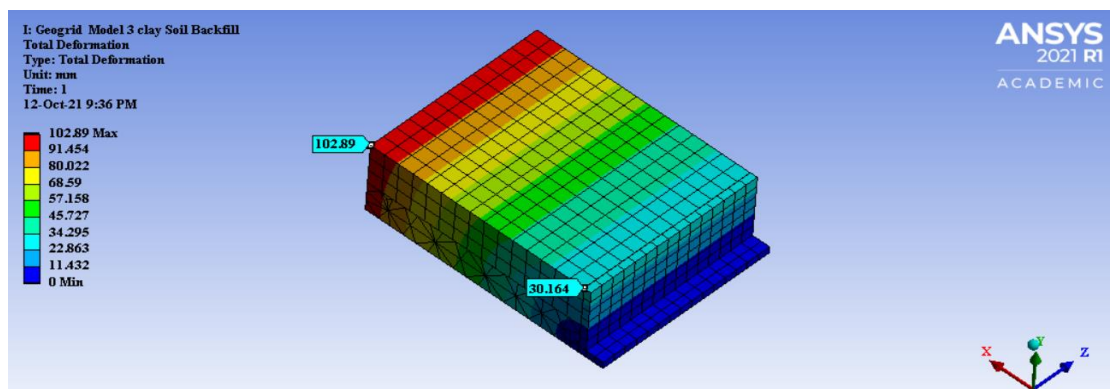


Fig. 17: Deformations result in model 3 with geogrid reinforcement

The retaining wall model with unreinforced well-graded soil i.e, model 1, when subjected to given loads, resulted in maximum deformation of 29.85 mm at the farthest point from the retaining wall and 8.80 mm at the face of the wall. When this model is reinforced with steel strips, the maximum deformation reduces by 52.3% and at the face of the wall, it is reduced by 52.7%. When the same model is reinforced with geogrid, the decrease in maximum deformation is 50.7% and at the wall face, deformation is decreased by 51.2%.

In model 2 i.e, retaining wall supporting poorly graded soil having no reinforcement at all, when subjected to given loads, resulting in maximum deformation of 259.95 mm at the farthest point and 76.65 mm at the wall face. When this model is reinforced with steel strips, maximum deformation is reduced by 54.7%, and at the face of the wall, its value decreased by 54.3%. In the same model, when the reinforcement is replaced with geogrids, the maximum deformation is reduced by 50.8% and deformation at the wall face is also reduced by 50.8%.

When model 3 i.e, retaining wall supporting clayey soil in unreinforced condition, subjected to given loads, the maximum deformations again occurred at the farthest point having the value of 240.56 mm and at the wall, face deformation was 70.83 mm. When the steel strips were used as reinforcement the maximum deformation was reduced by 60.9% and was reduced by 60.5% at the wall face. When the steel strips are replaced by geogrids, the maximum deformation and deformation at the wall face both decreased by 57.2%.

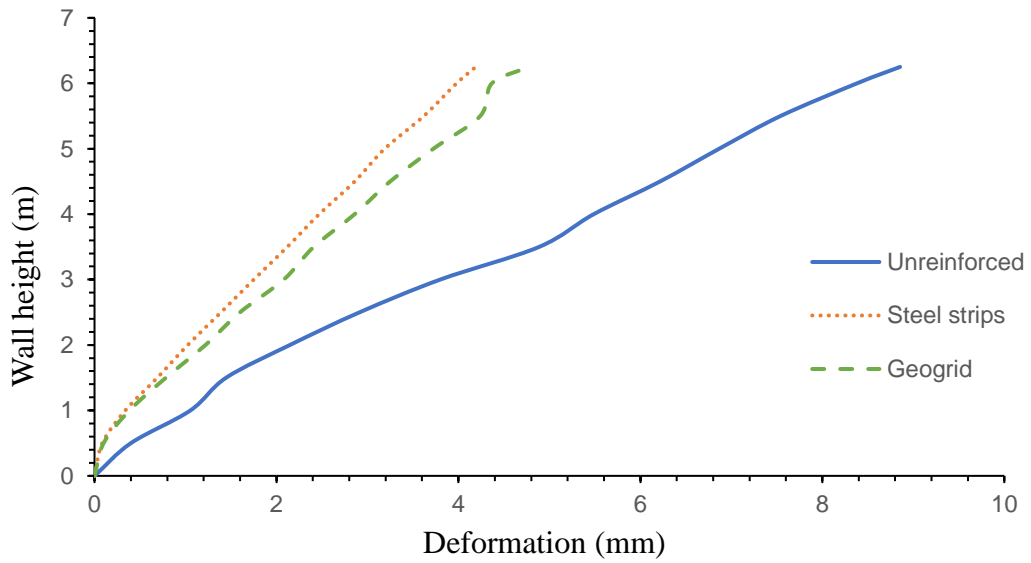
Table 9: Comparison of results of deformations in unreinforced and reinforced soil in different cases

Reinforcement	Model Parameters	Maximum Deformation in the backfill (mm)	Deformation at the top of the wall (mm)
Unreinforced	Well graded soil	29.85	8.80
	Poorly graded soil	259.95	76.65
	Clayey soil	240.56	70.83
Steel strips	Well graded soil	14.24	4.20
	Poorly graded soil	117.5	23.05
	Clayey soil	94.03	27.3

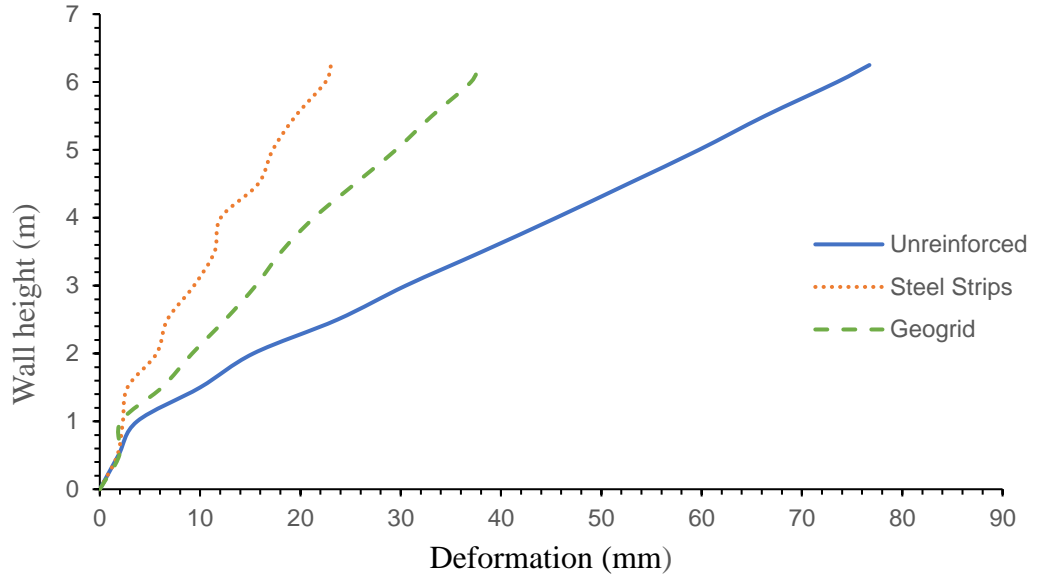
Geogrid	Well graded soil	16.19	4.77
	Poorly graded soil	128.47	37.8
	Clayey soil	102.89	30.16

Table 10: Comparison of the deformation of soil models with the steel strips and the geogrids

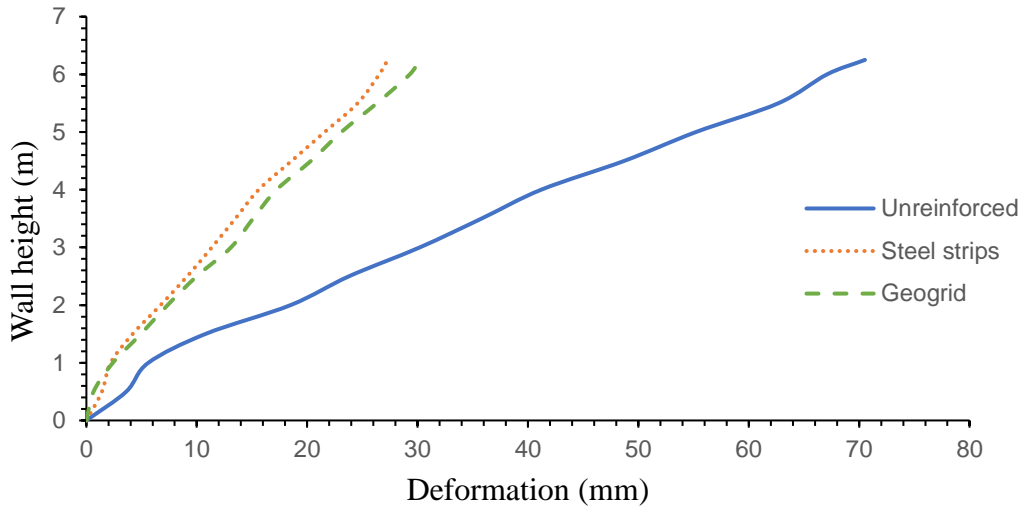
Condition	Steel Strips		Geogrid	
	Decrease in Maximum Deformation	Decrease in Deformation at top of the Wall	Decrease in Maximum Deformation	Decrease in Deformation at Wall
Well graded soil	52.3%	52.7%	50.7%	51.2%
Poorly graded soil	54.7%	54.3%	50.8%	50.8%
Clayey soil	60.9%	60.5%	57.2%	57.2%



(a) Well graded soil in unreinforced and reinforced condition



(b) Poorly graded soil in unreinforced and reinforced condition



(c) Clayey soil in unreinforced and reinforced condition

Fig. 18: Variation in the lateral deformation of the retaining wall with respect to wall height in different cases of the backfill in unreinforced and reinforced condition

From Fig. 18, it is clearly seen that the lateral deformations in the retaining wall with respect to its height are very large in the unreinforced condition in all three soil conditions. The introduction of the reinforcements into the soil has significantly reduced the lateral deformations in the wall.

#### 4.1.3 Comparison of $G/G_{\max}$ vs Density of Various Models

To understand the strength reduction in various models i.e, which model is most suitable and least suitable as per strength criteria, a comparison of  $G/G_{\max}$  vs Density is done for all three models.

According to Hardin and Black, the maximum value of shear modulus ( $G_{\max}$ ) for granular soils can be calculated by the following relation (Das, 1982) :

$$G_{\max} = \frac{3230 (2.97 - e)^2 (\sigma_0)^{1/2}}{1 + e} \quad (4.3)$$

where  $e$  = void ratio of backfill

$\sigma_0$  = Confining pressure in  $\text{N/m}^2$

Table 11: Typical values of void ratio for different types of soil (Das, 2008)

Type of soil	Void ratio( $e$ )	
	Minimum	Maximum
Well graded soil	0.26	0.74
Poorly graded soil	0.26	1.10
Sandy Clay soil	0.25	1.80

For  $e = 0.26$  and  $\sigma_0 = 2.5 \times 10^6 \text{ N/m}^2$  ,

$$G_{\max} = \frac{3230 (2.97 - 0.26)^2 (2.5 \times 10^6)^{1/2}}{1 + 0.26} = 30.12 \times 10^6 \text{ N/m}^2$$

For  $e = 0.95$  and  $\sigma_0 = 2.5 \times 10^6 \text{ N/m}^2$

$$G_{\max} = \frac{3230 (2.97 - 0.95)^2 (2.5 \times 10^6)^{1/2}}{1 + 0.95} = 6.4 \times 10^6 \text{ N/m}^2$$

According to Hardin and Drenvich, the maximum value of shear modulus ( $G_{\max}$ ) for cohesive soils can be calculated by the following relation (Das, 1982) :

$$G_{\max} = \frac{3230 (2.97 - e)^2 (\sigma_0)^{1/2} (\text{OCR})^p}{1 + e} \quad (4.4)$$

where,  $e$  = void ratio of backfill

$\sigma_0$  = Confining pressure in N/m<sup>2</sup>

OCR = Over consolidation ratio

The term P in Eq 4.4 is dependent on the plasticity index of soils.

Table 12: Values of P with variation of plasticity index (Das, 1982)

Plasticity index (%)	P
0	0
20	0.18
40	0.30
60	0.41
80	0.48
>100	0.5

Consider OCR = 1, Plasticity index = 40%, P = 0.30 in Eq 4.4

For e = 1.25 and  $\sigma_0 = 2.5 * 10^6 \frac{N}{m^2}$

$$G_{max} = \frac{3230 (2.97 - 1.25)^2 (2.5 * 10^6)^{1/2} (1)^{0.30}}{1 + 1.25} = 6.7 \times 10^6 \text{ N/m}^2$$

Table 13: Ratio of G and  $G_{max}$  with void ratio and density for different models

Model Parameters	Void ratio (adopted)	Density (KN/m <sup>3</sup> )	G (MPa) (adopted)	$G_{max}$ (MPa) (calculated)	$\frac{G}{G_{max}}$
Model 1 well graded backfill soil	0.26	20.4	30	30.1	0.99
Model 2 poorly graded backfill	0.95	19.4	3.1	6.4	0.48
Model 3 clay Soil Backfill	1.25	18.4	2.69	6.7	0.40

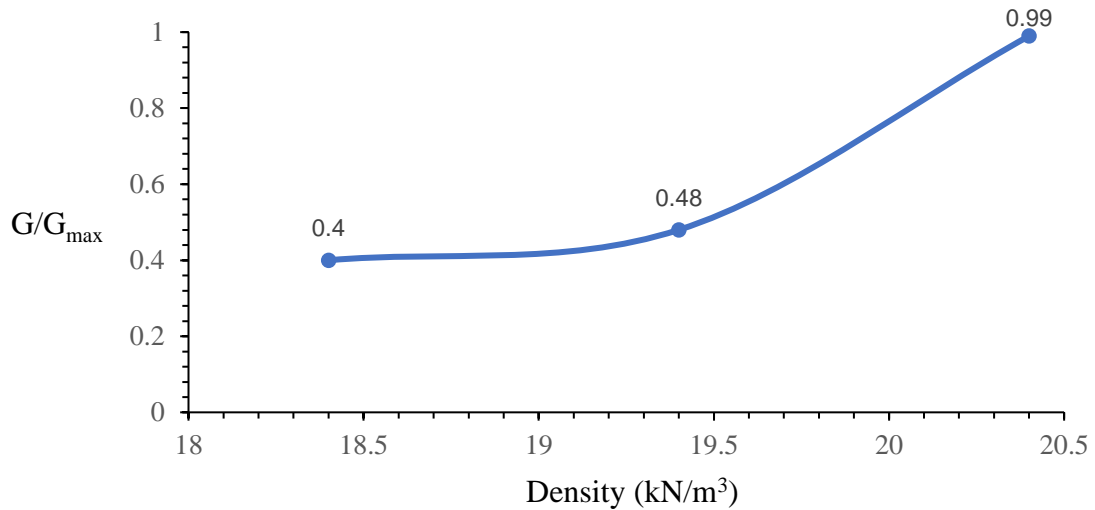


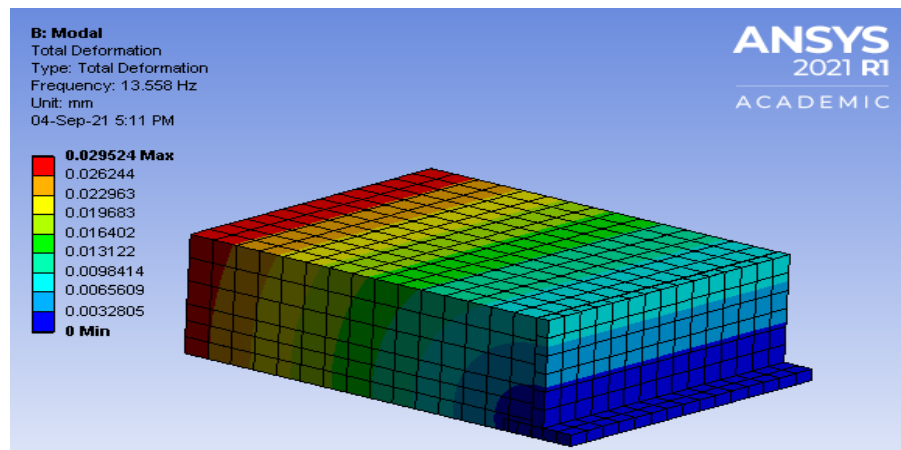
Fig. 19: Plot of  $G/G_{\max}$  vs Density of various models

Fig. 19 represents the strength reduction curve for different models. The higher the value of  $G/G_{\max}$ , the higher is the strength of the model. For model 1,  $G/G_{\max}$  value is 0.99, which is the maximum among the three models, indicating that the well-graded soil model is best in strength criteria whereas the  $G/G_{\max}$  value is minimum for model 3 indicating that the clayey soil model is having least strength.

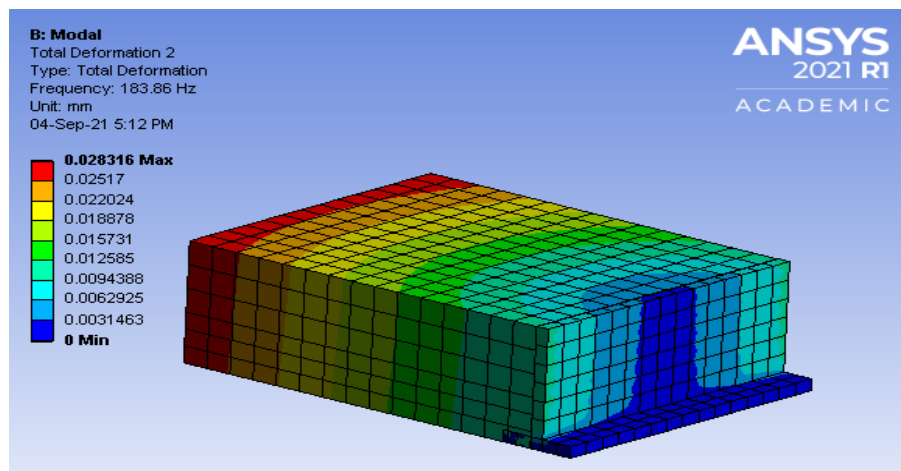
#### 4.1.4 Frequency Response Results of Retaining Wall

In this section, we try to investigate the frequency response of the retaining wall when a certain range of frequency and loads applied in a sinusoidal form to the system and also try to find out the resonant frequency of the retaining wall when dynamic loads in terms of force and frequency are applied to the system in different types of soils. For performing frequency response, modal analysis is the first step. So to perform modal analysis, simply drag the 'modal' under 'analysis settings' from 'toolbox' in the already prepared 'model' of static structural in Ansys. The benefit of dragging modal in 'model' of static structural is that we don't need to draw geometry and apply fixed support to the wall again. It will automatically link to it. Since this analysis does not require any load, so we directly obtained mode shapes and mode frequencies or natural frequencies of the system. Mode shapes are the motion patterns of a system vibrating or oscillating at its natural frequency and these natural frequencies are nothing but the mode frequencies. The motion patterns are random. Total 6 mode shapes and respective mode frequencies are calculated for models of retaining wall supporting well-graded, poorly graded, and clayey soil, and the results are shown below.

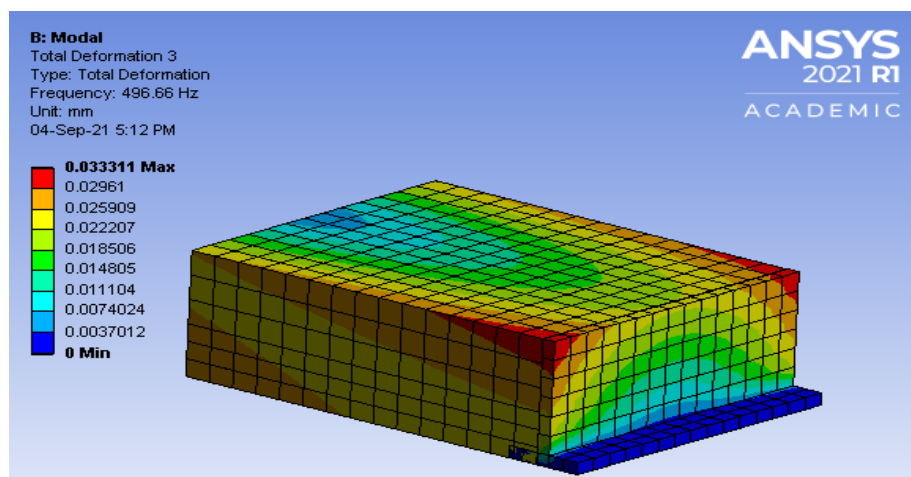
## Retaining wall supporting well-graded soil model



(a) Mode shape pattern at 13.55 Hz ( First mode frequency)

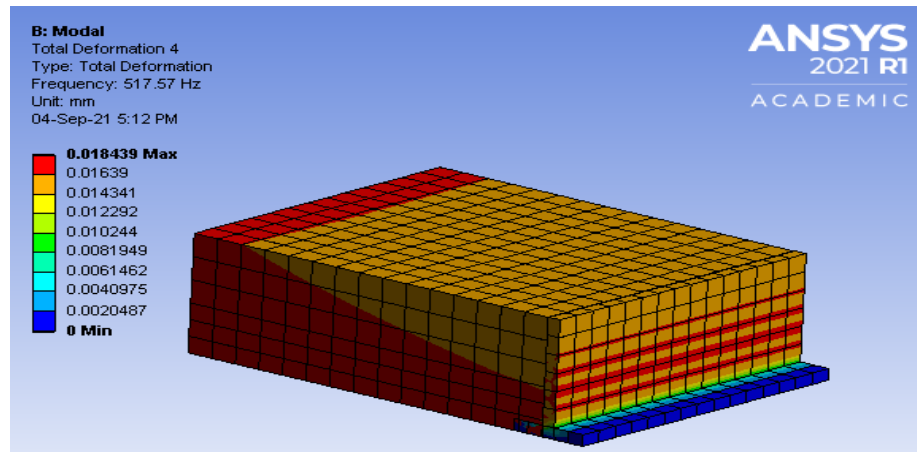


(b) Mode shape pattern at 183.86 Hz (Second mode frequency)

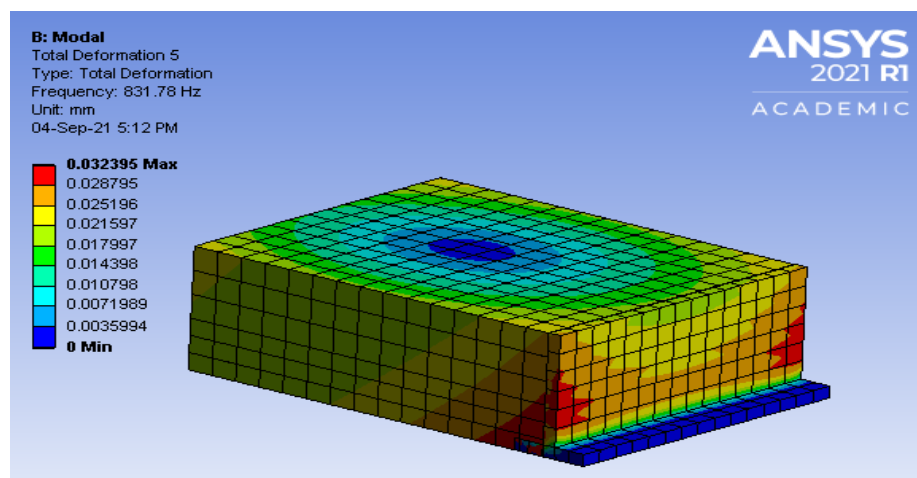


(c) Mode shape pattern at 496.66 Hz (Third mode frequency)

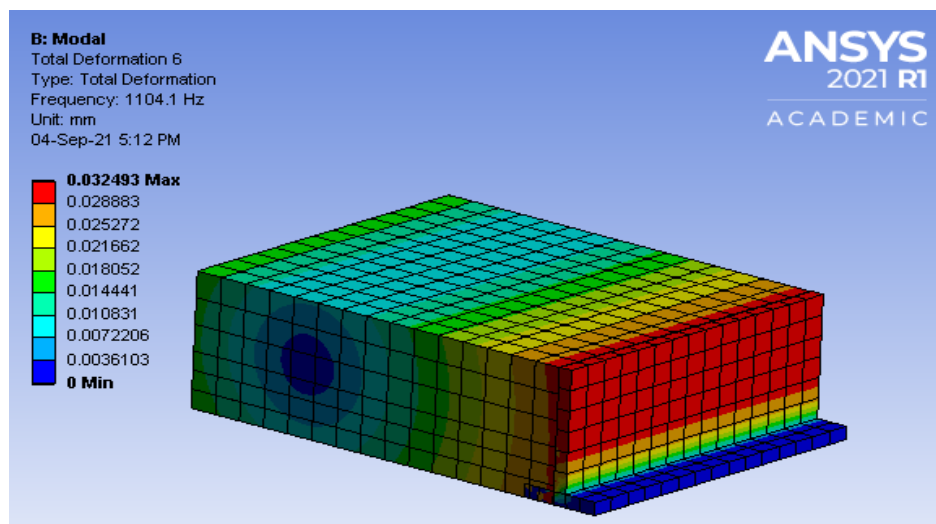




(d) Mode shape pattern at 517.57 Hz (Fourth mode frequency)



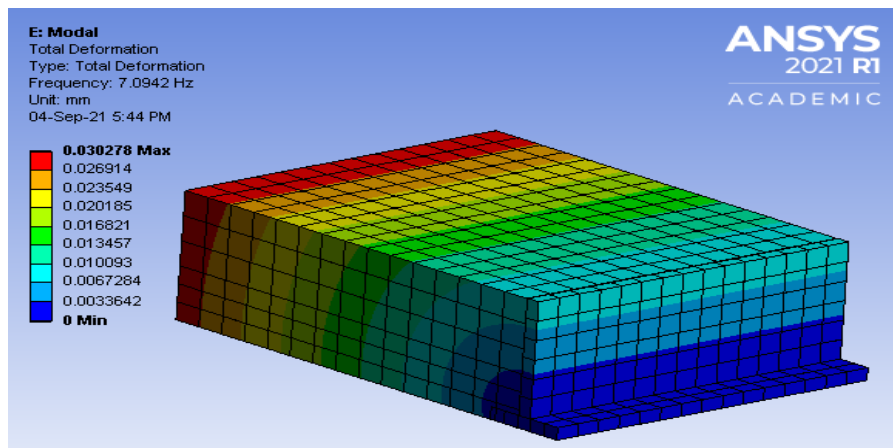
(e) Mode shape pattern at 831.78Hz (Fifth mode frequency)



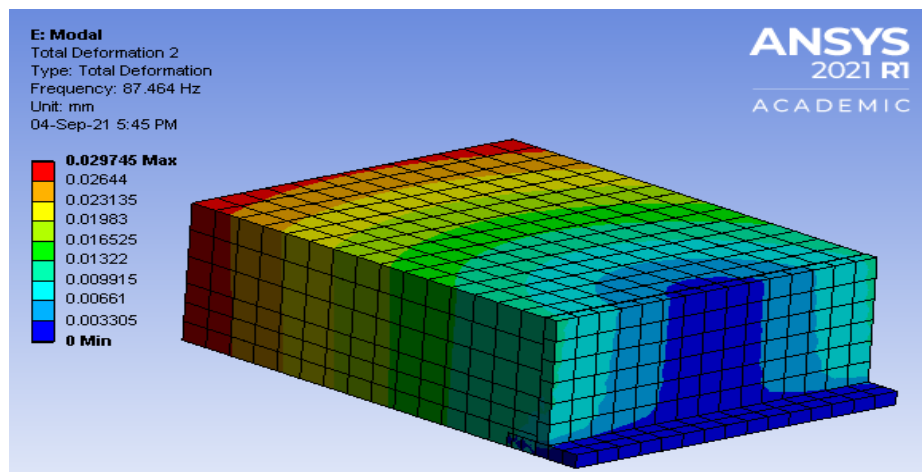
(f) Mode shape pattern at 1104.1 Hz (Sixth mode frequency)

Fig. 20: Mode shape patterns with respective mode frequency for well-graded soil

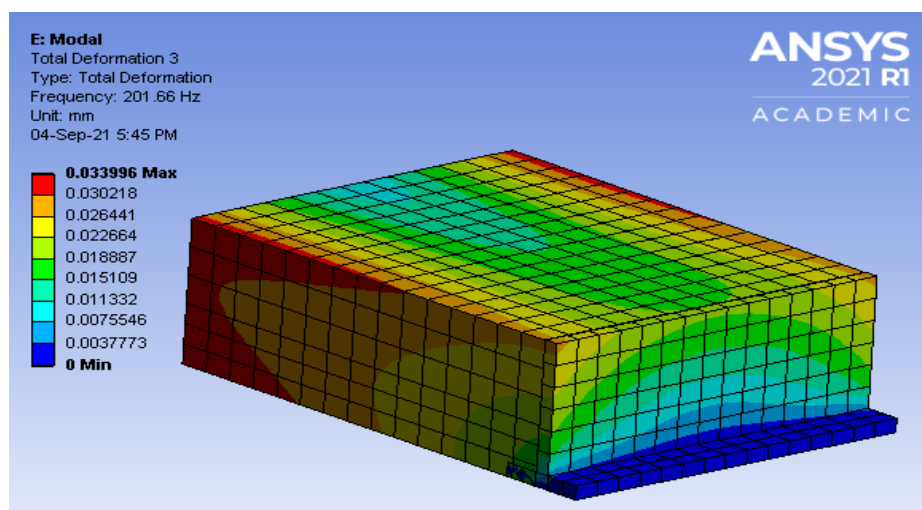
## Retaining wall supporting poorly graded soil model



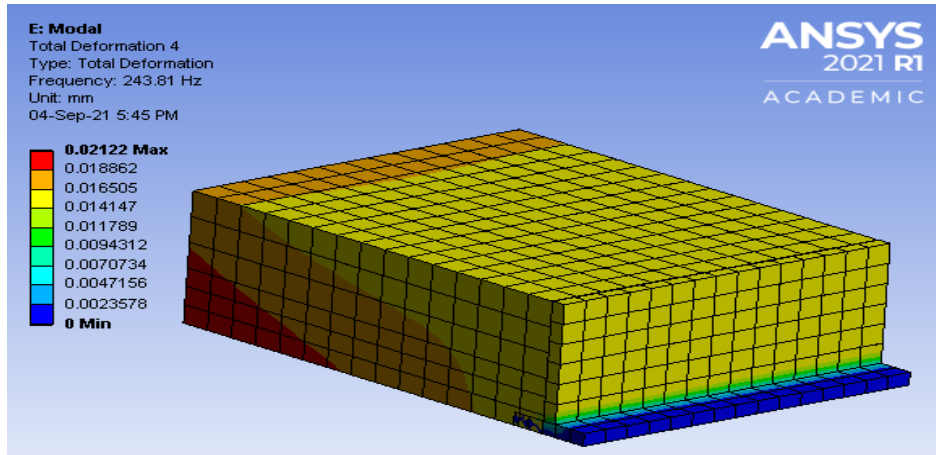
(a) Mode shape pattern at 7.09 Hz ( First mode frequency)



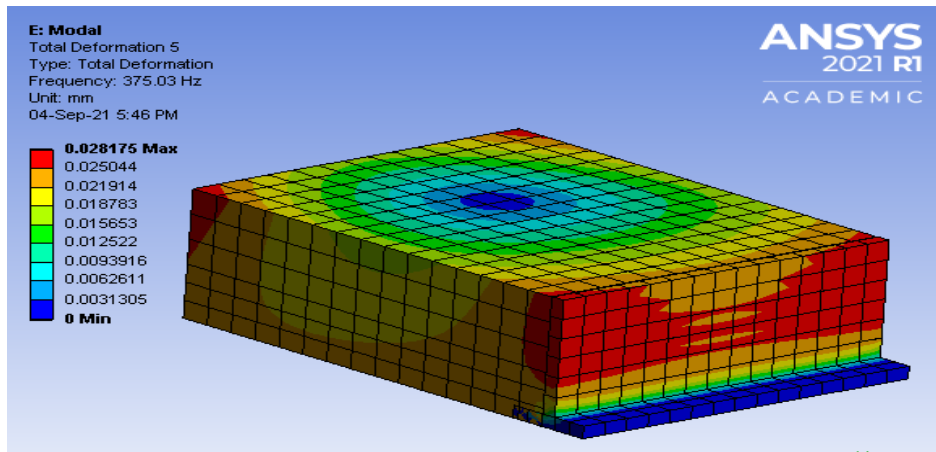
(b) Mode shape pattern at 87.46 Hz (Second mode frequency)



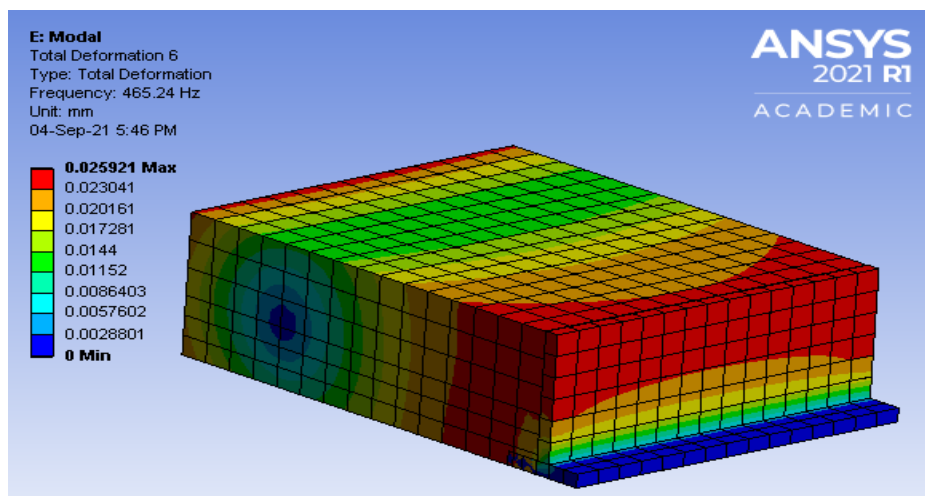
(c) Mode shape pattern at 201.66 Hz (Third mode frequency)



(d) Mode shape pattern at 243.81 Hz (Fourth mode frequency)



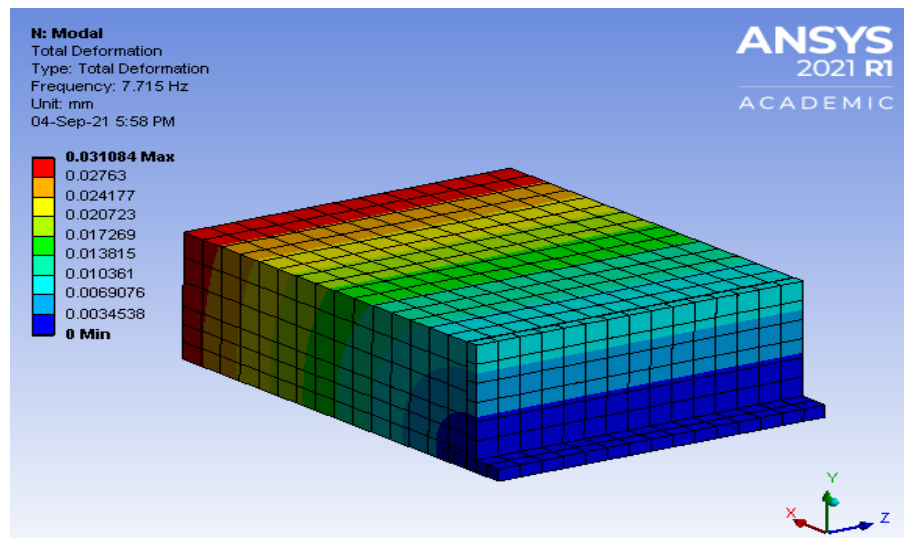
(e) Mode shape pattern at 375.03 Hz (Fifth mode frequency)



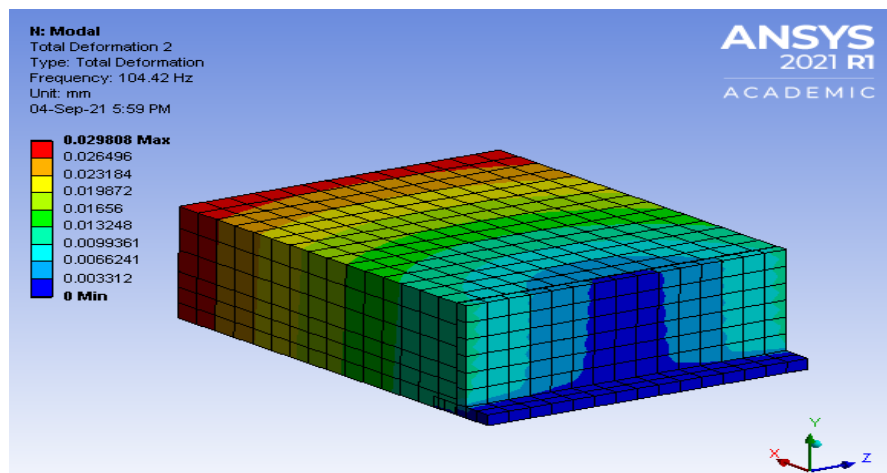
(f) Mode shape pattern at 465.24 Hz (Sixth mode frequency)

Fig. 21: Mode shape patterns with respective mode frequency for poorly graded soil

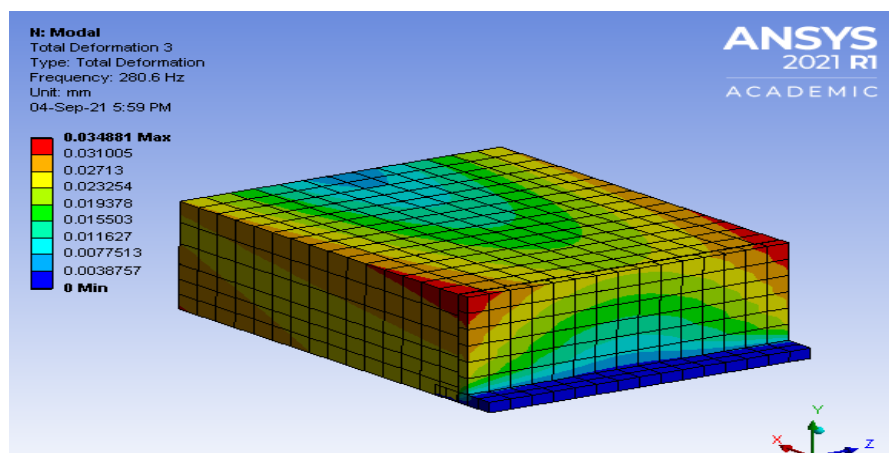
## Retaining wall supporting clayey soil model



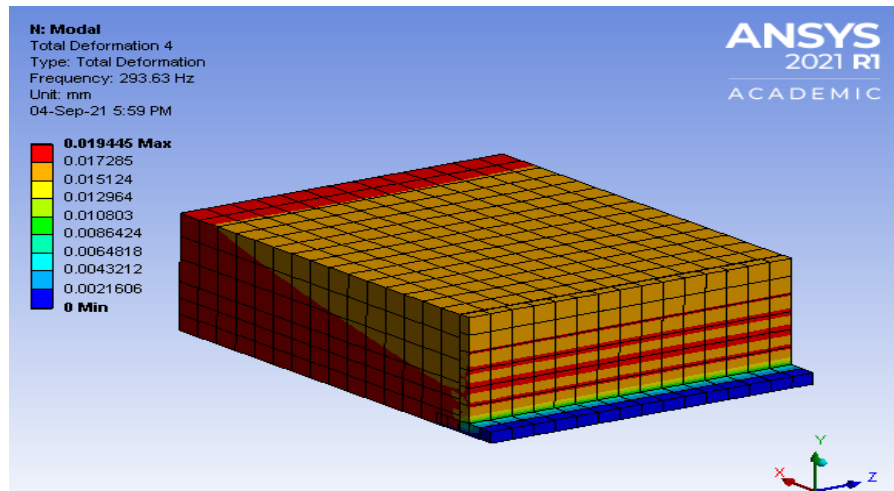
(a) Mode shape pattern at 7.71 Hz ( First mode frequency)



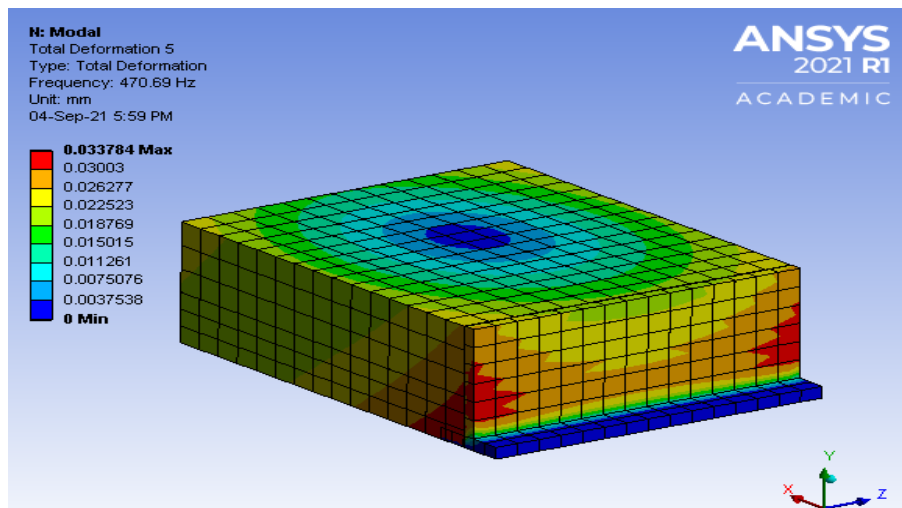
(b) Mode shape pattern at 104.42 Hz (Second mode frequency)



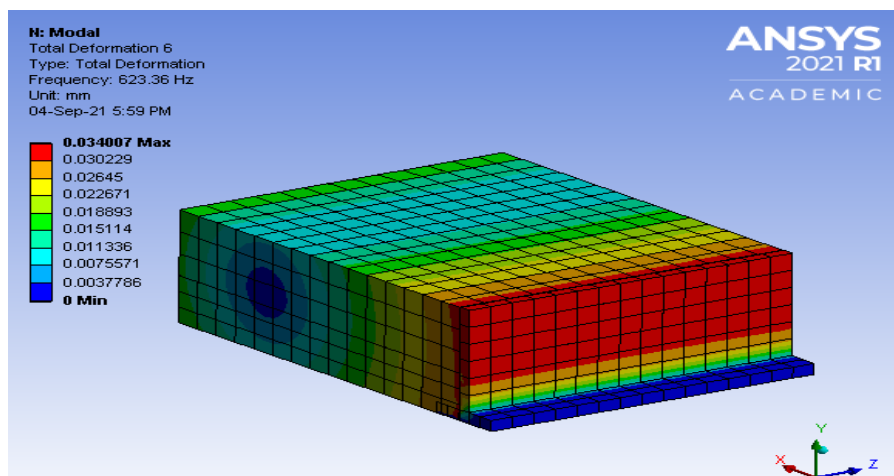
(c) Mode shape pattern at 280.6 Hz (Third mode frequency)



(d) Mode shape pattern at 293.63 Hz (Fourth mode frequency)



(e) Mode shape pattern at 470.6Hz (Fifth mode frequency)



(f) Mode shape pattern at 623.36 Hz (Sixth mode frequency)

Fig. 22: Mode shape patterns with respective mode frequency for clayey soil

When a component vibrates at its natural frequency, its mode shape characterizes the deformation it will exhibit. Fig 20 shows the mode shape patterns of the model of the retaining wall supporting well-graded soil with their respective mode frequencies. Mode shape patterns and respective mode frequencies for other cases like for retaining wall supporting poorly graded soil model and for retaining wall supporting clayey soil model are shown in Fig. 21 and Fig. 22, respectively. For retaining wall supporting well-graded soil, the first six natural frequencies are 13.5 Hz, 183.86 Hz, 496.66 Hz, 517.57 Hz, 831.78 Hz, and 1104.1 Hz respectively. For retaining wall supporting poorly graded soil, the first six natural frequencies are 7.09 Hz, 87.46 Hz, 201.66 Hz, 243.81 Hz, 375.03 Hz, and 465.24 Hz respectively. For retaining wall supporting clayey soil, the first six natural frequencies are 7.71 Hz, 104.42 Hz, 280.6 Hz, 293.63 Hz, 470.69 Hz, and 623.36 Hz.

Table 14: Different models and their mode frequencies

Model Parameters	Natural or Mode Frequencies (Hz)					
	1 <sup>st</sup> mode	2 <sup>nd</sup> mode	3 <sup>rd</sup> mode	4 <sup>th</sup> mode	5 <sup>th</sup> mode	6 <sup>th</sup> mode
Well graded soil	13.55	183.86	496.66	517.57	831.78	1104.1
Poorly graded soil	7.09	87.46	201.66	243.81	375.03	465.24
Clayey soil	7.715	104.42	280.64	293.63	470.69	623.36

Table 15: The first fundamental frequency of the retaining wall predicted by various researchers

Name	1st natural frequency (Hz)
Elgamal et al.(1996)	5.8
Darvishpour et al. (2017)	4.3
Hatami et al (2018)	5.1

Table 16: The first fundamental frequency of the retaining wall by the current study

Type of model	1 <sup>st</sup> natural frequency (Hz)
Model 1 well-graded backfill soil	13.5
Model 2 poorly graded backfill	7.09
Model 3 clay Soil Backfill	7.7

The first fundamental frequency predicted by various researchers in Table 16 is less than 6 Hz in all the cases. But for this study, the first fundamental frequency of the retaining wall in all the three cases of the soil considered is in the range of 7–13.5 Hz which shows that the considered models are stiffer and less prone to deformations and damages under vibrations and can be used for realistic purpose also.

After obtaining six mode results, we have six natural frequencies. We need to test that how our system will behave, how much deformation we get if we excite our system by inserting these natural frequencies as input frequencies. Harmonic response or frequency response analysis can solve this issue. So for harmonic response, drag ‘harmonic response’ under ‘analysis settings’ from ‘toolbox’ in ‘model’ of modal analysis. The ‘engineering data’ and ‘geometry’ will get automatically linked. First, apply for fixed support at the base of the wall. The force is then applied to the system in sinusoidal form having a frequency sweep of 1-1000 Hz.

Let the gross weight of a car,  $M$  = self-weight + weight of persons sitting in the vehicle

$$= 10,000 \text{ kg} + 500\text{kg}$$

$$M = 10,500 \text{ kg}$$

Now from the standard force equation,

$$F = \text{Mass (M)} \times \text{Acceleration (a)} \quad (4.5)$$

The average rate of acceleration for petrol cars is  $0.64 \text{ m/s}^2$  (Bokare, 2017) , therefore,

$$F = 10,500 \times 0.64 = 6,720 \text{ N}$$

Force equation in sinusoidal form is given as,

$$F = F_0 \sin \omega t \quad (4.6)$$

where  $F_0$  is maximum amplitude which is taken here as 6,720 N

$t$  = time in seconds

$\omega$  = angular frequency in rad / sec

Table 17: The values of force amplitude in newtons for exciting angular frequencies in radians/second

Angular Frequency (in rad / sec)	Force (in Newtons)
100	-3402
200	-5868
300	-6718
400	-5718
500	-3143
600	296
700	3655
800	6007
900	6705
1000	5556

In Table 17, for simplicity purposes, the values of angular frequency and thus force amplitude are shown in multiples of 100 but in simulation software, it is taken as 1 to 1000 units in tabular form. Now after we have applied fixed support, pressure, and force, the next step is to obtain the frequency response of the retaining wall. So from 'solutions' go to 'frequency response', select 'displacement' then in geometry select the object that is for we want frequency response, i.e, the retaining wall.



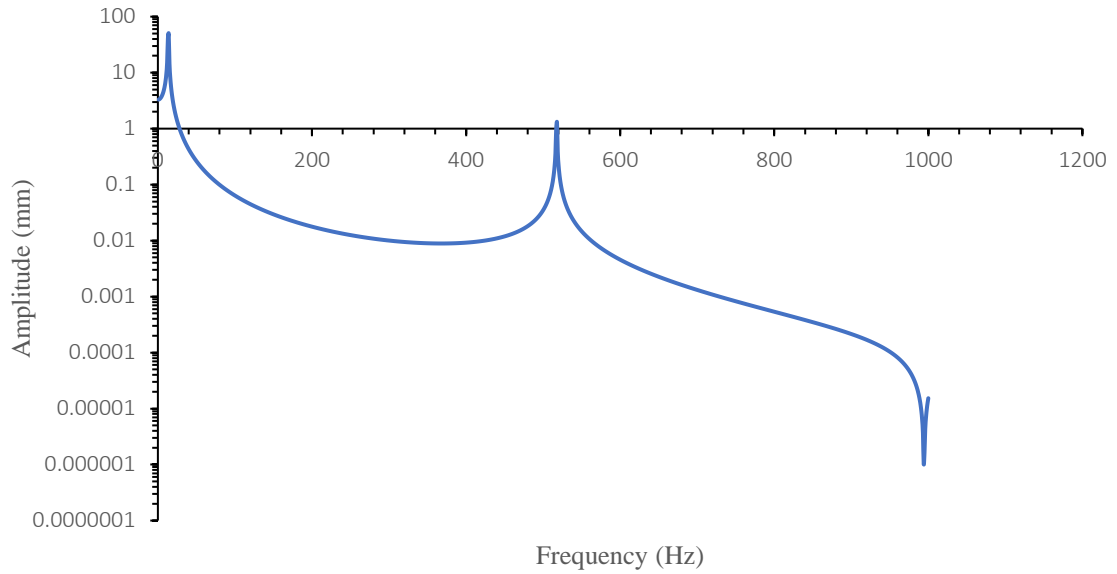


Fig. 23: Frequency response analysis of displacement for retaining wall supporting well-graded soil in semi-log scale

From modal analysis, we know that 13.5 Hz is the first natural frequency for retaining wall supporting well-graded soil that means if we excite our model by this input frequency then our system possibly has horrendous vibrations and amplitude might reach its maximum value, called resonance condition. This leads to irreparable damage. Fig 23 depicts that from 1 to 11 Hz, the amplitude is increasing gradually from 3.3 mm to 9 mm. When the system is excited at 12 Hz, the amplitude is 15 mm i.e, a short jump in amplitude can be seen but when the system is excited at 13 Hz, the amplitude is skyrocketed and lands on 40.7 mm amplitude mark, and at 14 Hz reaches its maximum value to 49.61 mm and then gradually goes on decreasing till 425 Hz. So we can clearly state from this frequency response analysis that at 14 Hz retaining wall supporting well-graded soil has a maximum amplitude and thus reaches resonance. So for this model, the resonant frequency is 14 Hz.

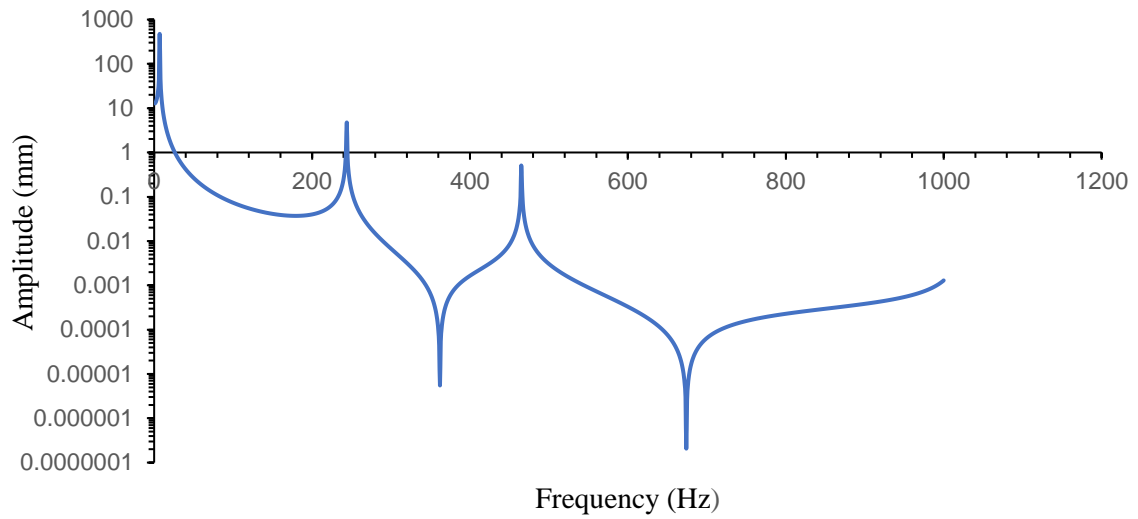


Fig. 24: Frequency response analysis of displacement for retaining wall supporting poorly graded soil in semi-log scale

From modal analysis, the first natural frequency for retaining walls supporting poorly graded soil is 7.09 Hz. Fig 24 shows that the amplitude progressively increases from 12.7 mm to 24.9 mm from 1 to 5 Hz. When the system is excited at 6 Hz, there is a leap in amplitude and the amplitude is 44.0 mm, but when the system is excited at 7 Hz, the amplitude value is 475.35 mm, which climbs 10 times and then progressively decreases until it reaches 180 Hz. As a result, the resonance condition was attained at 7 Hz.

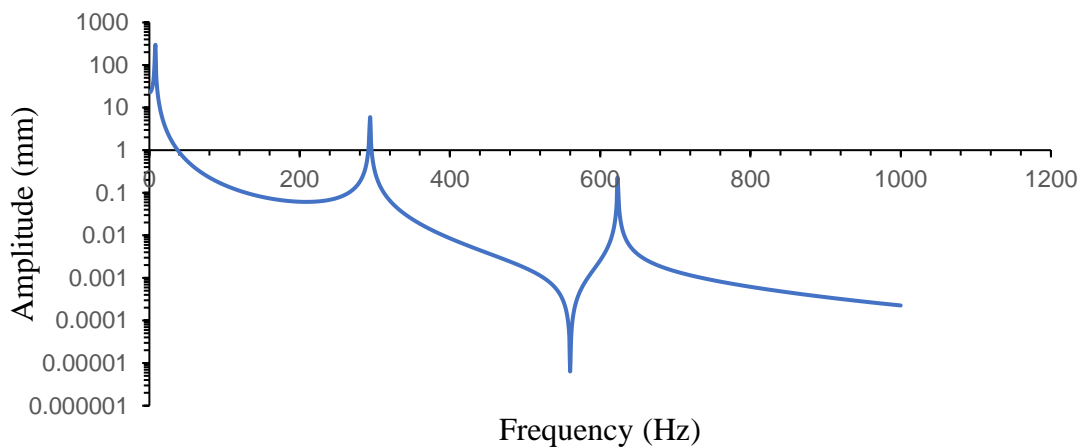


Fig. 25: Frequency response analysis of displacement for retaining wall supporting clayey soil in semi-log scale

As per modal analysis, 7.7 Hz is the first natural frequency for retaining walls supporting clayey soil. The amplitude increases from 22.8 mm to 38.7 mm from 1 to 5 Hz, as seen in Fig 25. When the system is stimulated at 6 Hz, there is a jump in amplitude and the amplitude is 56.9 mm, but when the system is excited at 7 Hz, the amplitude practically doubles to 127.2 mm, and at 8 Hz, it achieves its highest value of 299.01 mm and then progressively decreases until 209 Hz. As a result, the resonance frequency for this model is 8 Hz.

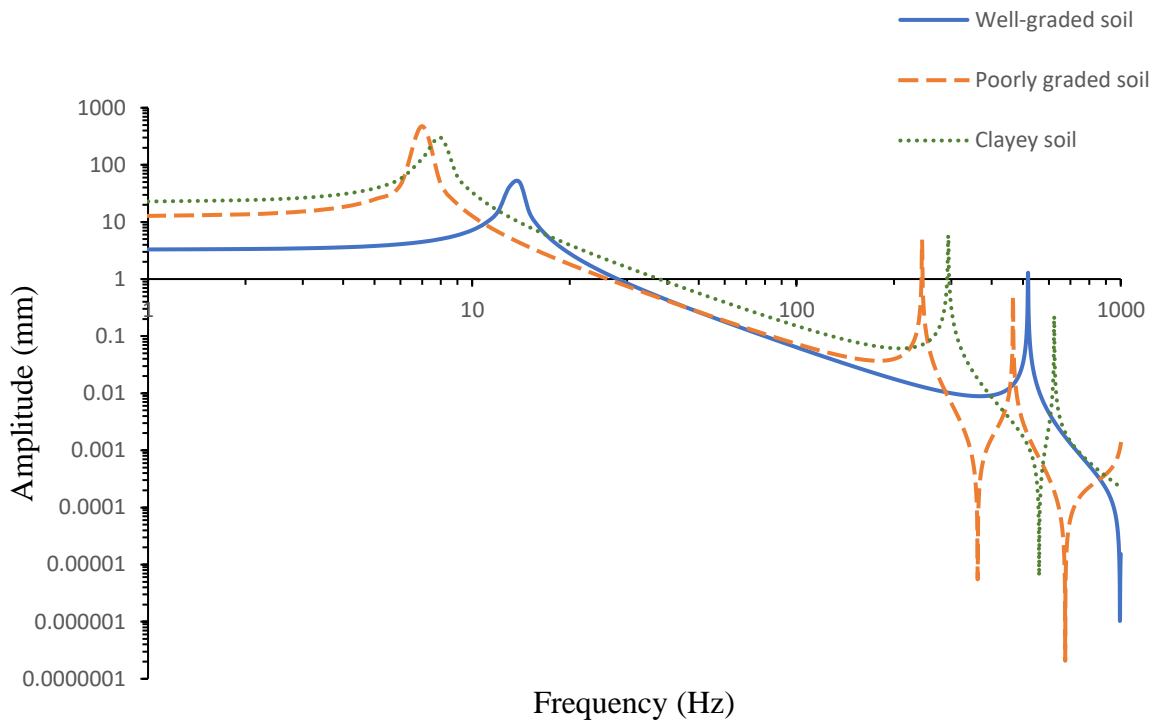


Fig. 26: Comparison of frequency response analysis of displacement for retaining wall supporting well-graded, poorly graded, and clayey soil in log-log scale

Fig. 26 depicts that for all the conditions of the soil, the amplitude of the displacement increases at a slow rate. At a certain frequency, there is a small jump in the amplitude of the displacement. This jump in the amplitude occurs at a different frequency for different cases. As we increase the input frequency, there is a shoot-up in the amplitude in all the cases and a maximum amplitude value is attained which marks the peak of the curve in all the respective cases. This peak in the amplitude is first reached in the retaining wall supporting poorly graded soil model at 7 Hz which states that the resonance condition is first attained in this model so it is more susceptible to damages than the other two cases. For retaining wall supporting well-graded soil model, the peak

in the amplitude is reached at the highest frequency among the three models i.e, at 14 Hz which means that this model is stiffer than the other two conditions of the models. There is no significant effect on the retaining wall of low amplitude deformation values because deformation occurs due to applied force in terms of energy and energy is square of amplitude. So low amplitude deformations like 0.001 mm will become 0.000001 mm which is almost zero. Therefore, no effect in terms of deformations in retaining wall.

## **CHAPTER 5**

### **CONCLUSION AND RECOMMENDATIONS FOR FUTURE WORK**

#### **CONCLUSION**

The numerical investigations on retaining wall are conducted using a finite element modeling program. The following conclusions are drawn on the basis of the test results.

- 1) The maximum deformation in the infill material and the lateral deformation at the top of the retaining wall were observed to be in the range of 29.85 - 240.56 mm and 8.8 - 70.83 mm respectively, for the set of selected parameters in the study.
- 2) The inclusion of reinforcement in backfill material decreased the maximum and interface deformation upto 60%.
- 3) The spacing between the reinforcement layers should be adequate (700 mm is taken). If the spacing between the reinforcing layers is too small, additional layers are required, increasing the overall cost and construction time. However, if the spacing is too high, then there is no meaningful reduction in deformations.
- 4) When the length of the reinforcement exceeds a certain value (here, 4,375 mm is taken), there is a reinforcement excess and the excess reinforcement is of no use, only it increases the cost of the construction.
- 5) From numerical simulations, it is found that steel strips despite having a stiffness value 40 times greater than geogrids, exhibited similar deformations results compared to geogrid with a negligible difference. Therefore, it is concluded that geogrid is more efficient in reducing deformations than steel strips.
- 6) From the frequency response results, it is concluded that the retaining wall supporting the well-graded soil model is stiffer as it shows higher resonant frequency (14 Hz) than the other two cases (7 Hz and 8 Hz, respectively).
- 7) The retaining wall supporting poorly graded soil is more prone to damages than the rest two cases as it shows the least resonant frequency (i.e, 7 Hz) among the three models and also the deformations are very large at the resonant frequency in the retaining wall.

## **RECOMMENDATIONS FOR FUTURE WORK**

1. This study does not consider the effect of the water table in the analysis. So numerical investigations on the retaining wall can be performed considering the effect of the water table at different positions of the backfill.
2. This study involves numerical investigations on the retaining wall with three types of soil as three different models. Similar studies can be done, considering different types of soils in the same model.
3. Analysis by the inclusion of reinforcement in frequency response study can be done.
4. The positions and spacing of the reinforcements play a key role in the analysis. So studies can be performed by changing the positions and spacing (horizontal or vertical or both) of the reinforcements.

## REFERENCES

1. Bokare, P.S., Maurya, A.K., (2017). Acceleration deceleration behavior of various vehicle types. *Transportation Research Procedia*, Volume 25, 4733-4749.
2. Cai, Z., and Bathurst, R.J., (1995). Seismic response analysis of geosynthetic reinforced soil segmental retaining walls by finite element method. *Computers and Geotechnics*, Volume: 17, 523-546.
3. Cakir, T., (2012). Evaluation of the effect of earthquake frequency content on seismic behavior of cantilever retaining wall including soil-structure interaction. *Soil Dynamics And Earthquake Engineering*, Volume 45, 96-111.
4. Cakir, T., (2015). Dynamic analysis of a cantilever retaining wall including soil-structure interaction. *Digital Proceeding of International Conference on Civil and Environmental Engineering*, 1289-1295.
5. Capilleri, P.P., Ferraiolo, F., Motta, E., Scotto, M., and Todaro, M., (2019). Static and dynamic analysis of two mechanically stabilized earth walls. *Geosynthetics International*, Volume: 26(1), 26-41.
6. Chowdhury, I., and Singh, J.P., (2015). Behavior of gravity type retaining wall under earthquake load with generalized backfill. *Journal of Earthquake Engineering*, Volume 19(4), 563-591.
7. Darvishpour, A., Ghanbari, A., Hosseini, S.A.A., (2017). A 3D analytical approach for determining natural frequency of retaining walls. *International Journal of Civil Engineering*, Volume 15, 363–375.
8. Das, B.M., (2016). Use of geogrid in the construction of railroads. *Innovative Infrastructure Solutions*, 1:15, 1-12.
9. Das, B.M., *Advanced Soil Mechanics* (2008). Taylor and Francis, London & New York, ISBN: 9781351215183.
10. Das, B.M., *Fundamentals of soil dynamics* (1982), Ch 2 - Stress waves in bounded elastic medium, 58-63, ISBN: 9780444007056.
11. Dongare, S.P., Gandhi, P.R., Gosavi, S.S., Redkar, P.A., Shaikh, R., (2019). Study on comparative design of retaining wall structures and analysis it in Ansys APDL

- Software. *International Research Journal of Engineering and Technology*, Volume 6(4), 3383-3393
12. Elgamal, A.W., Alampalli, S., and Laak, P.V., (1996). Forced vibration of full-scale wall-backfill system. *Journal of Geotechnical Engineering*, 122(10), 849-858.
  13. Hussaini, S.K.K., Kumari, S., (2021). Investigation of deformation and degradation response of geogrid-reinforced ballast based on model track tests. *Proceedings of the Institution of Mechanical Engineers, Part F: Journal of Rail and Rapid Transit*, 235(4), 505-517.
  14. Khati, B.S., Saran, S., Mukerjee, S., Kumar, D., (2012). Effect of embedment and geogrid reinforcement on dynamic elastic properties of silty sand. *International Journal Of Engineering Research & Technology*, Volume 1(8), 1-8
  15. Komakpanah, A., Yazdi, M., (2012). Frequency response analysis of reinforced-soil retaining walls with polymeric strips. *International Journal of Civil and Environmental Engineering*, Volume: 6(3), 261-266.
  16. Langcuyan, C.P., Gao, Y., and Won, M.S., (2018). Effects of surface vibrations on the behavior of panel-type MSE walls. *World Congress on Advances in Civil, Environmental, & Materials Research (ACEM18)*.
  17. Li, L., Yang, J., Xiao, H., Zhang, L., Hu, Z., and Liu, Y., (2020). Behavior of tire-geogrid-reinforced retaining wall system under dynamic vehicle load. *International Journal of Geomechanics*, Volume 20(4): 04020017.
  18. Ling, H.I., Victor, H.L., Kaliakin, N., and Leshchinsky, D., (2004). Analyzing dynamic behavior of geosynthetic-reinforced soil retaining walls. *Journal of Engineering Mechanics*, Volume 130(8): 911-920.
  19. Nicholson, P.G., (2015). Soil improvement and ground modification methods. Elsevier Inc, ISBN: 978-0-12-408076-8.
  20. Patel, A., (2019). Soil reinforcement, geotechnical investigations and improvement of ground conditions. Elsevier Inc, ISBN: 978-0-12-817049-6.
  21. Qiu, C.C., Lin, Y.L., Ma, Y., He, M., and Hong, S.J., (2019). Effect of vibration frequency on settlement characteristic of reinforced embankment by geogrid with strengthened nodes using DEM simulation. *International Conference on Numerical Modeling in Engineering*, 657, 012016, 1-8.
  22. Safaei, A.M., Mahboubi, A., Noorzad, A., (2020). Experimental investigation on the performance of multi-tiered geogrid mechanically stabilized earth (MSE) walls



- with wrap-around facing subjected to earthquake loading. *Geotextiles and Geomembranes*, Volume 49, 130-145.
23. Samal, M. R., Saran, S., Kumar, A., and Mukerjee, S., (2016). Dynamic behavior of geogrid reinforced pond ash. *International Journal of Geotechnical Engineering*, Volume 10(2), 114-122.
  24. Sridevi, G., Shivaraj, A., and Sudarshan, G. (2021). Seismic stability of retaining wall with and without geogrid inclusions in the backfill. *Proceedings of the Indian Geotechnical Conference*, Volume 138, 885-899.
  25. Tarawneh, B., Bodour, W.A.L., and Masada, T., (2018). Inspection and risk assessment of mechanically stabilized earth walls supporting bridge abutments. *Journal of Performance of Constructed Facilities*, Volume 32(1): 04017131.
  26. Tuan, C.Y., (2014). Ground shock resistance of mechanically stabilized earth walls. *International Journal of Geomechanics*, Volume 14(3): 06014003.
  27. Wang, L., Chen, G., Chen, S., (2014). Experimental study on seismic response of geogrid reinforced rigid retaining walls with saturated backfill sand. *Geotextiles and Geomembranes*, Volume 43, 35-45.
  28. Xu, P., Hatami K., and Li, T., (2019). Natural frequency of full-height panel reinforced soil walls of variable cross-section. *Geosynthetics International*, Volume 26(3), 320-331.
  29. Yang, G.Q., Lv, P., Zhang, B.J., Zhou, Q.Y., (2008). Study on the geogrid reinforced soil retaining wall of concrete rigid face by field test. *Geosynthetics in Civil and Environmental Engineering*, pp 255-260.
  30. Yazdandoust, M., (2017). Investigation on the seismic performance of steel-strip reinforced-soil retaining walls using shaking table test. *Soil Dynamics and Earthquake Engineering*, Volume 97, 216–232.
  31. Yazdandoust, M., (2018). Laboratory evaluation of dynamic behavior of steel-strip mechanically stabilized earth walls. *Soils and Foundations*, Volume 58(2), 264-276.
  32. Yu, Y., Bathurst, R. J. and Allen, T. M. (2017). Numerical modeling of two full-scale reinforced soil wrapped-face walls. *Geotextiles and Geomembranes*, Volume 45(4), 237–249.
  33. Yu, Y., Bathurst, R.J., Miyata, Y., (2015). Numerical analysis of a mechanically stabilized earthwall reinforced with steel strips. *Soils and Foundations*, Volume 55(3), 536-547.